Mantle sources of ocean islands basalts revealed from noble gas isotope systematics

James M.D. Day*, Tim D. Jones, Robert W. Nicklas

Scripps Institution of Oceanography, University of California San Diego, La Jolla, CA 92093-0244
*Corresponding author: jmdday@ucsd.edu

Special Volume in honor of **David R. Hilton for *Chemical Geology,*** *submitted: April 17 2021; revision submitted August 26 2021*

Abstract length: 403

Word Count: 9906

Figures: 16

Tables: 2

Keywords: Ocean island; basalt; helium; neon; argon; xenon; deep mantle; depletion; recycling

Abstract:

Noble gas isotope systematics, particular those of He, have been fundamental in showing that some ocean island basalts (OIB) were sourced from deep mantle plumes. Relationships between He, W, Os, Sr, Nd and Pb isotopes in Hawaiian, Samoan, Galapagos, and Icelandic lavas have been suggested to reflect contributions from less degassed lower mantle sources, and perhaps even materials advected from the core-mantle boundary. This study reviews the noble gas (He-Ne-Ar-Xe) isotope systematics of major OIB suites. Important in this evaluation are considerations of spatial and temporal variations, including the sample media (glass, minerals, hydrothermal gases and fluids) used for analyzing noble gases, as well as the degree of partial melting experienced to produce OIB. Limited availability of gas-rich samples means patchy coverage in definition of OIB Ne, Ar, Xe isotope compositions. Additionally, low-degree partial melting will lead to preferential sampling of more fusible, generally more enriched components which could affect noble gas isotope systematics. OIB with low- (<8R_A) to MORB-like $^3He/^4He$ (8±2R_A) dominantly sample convecting mantle domains and can also contain some relatively undegassed (solar) components. Their range in Sr-Nd-Os-Pb isotope compositions reflect a strongly recycled crustal and/or lithospheric heritage. Intermediate (>10R_A) to high-$^3He/^4He$ (>25R_A) OIB (Loihi, Hawaii; Iceland; Fernandina, Galapagos; Ofu, Samoa) sample a reservoir that has been relatively isolated since ~4.5 billion years as shown by noble gases (He, Ne, Ar, Xe), and by W isotopes. However, this reservoir is not pristine and these OIB show evidence for containing depleted and enriched recycled components from Xe isotopes as well as lithophile-siderophile radiogenic isotope systematics. Linking the highest-$^3He/^4He$ OIB to a putative Focus Zone (FOZO) reservoir is also problematic; FOZO is not a reservoir least affected by recycling of crust, rather a mantle reservoir that contains recycled components, including depleted lithosphere, and that has been oxidized. This distinction in definition means that, while the FOZO reservoir is almost certainly sampled by the deepest, hottest mantle plumes, its status as a primitive reservoir is unsubstantiated. Models of mantle convection can satisfy seismic constraints on Earth's deep mantle and reveal extensive mixing throughout with enriched and depleted lithologies formed by partial melting processes at Earth's surface. Ancient deep isolated reservoirs are likely to be relatively minor present-day mantle features. More remarkable is the predicted abundance of strongly refractory mantle material. Focus on the noble gas, radiogenic and stable isotope attributes of such refractory reservoirs are required for a fuller understanding of mantle processes.

1. Introduction

The noble gases are powerful geochemical tools in the study of Earth's accretion, differentiation and structure. Several reasons exist for this utility, chief amongst them being the chemical inertness of the noble gases at Earth's surface, having full orbital electron shells surrounding their nucleus. The noble gases span a wide range of atomic mass, from He (3 amu) to Xe (136 amu) (**Table 1**). These mass differences, together with the 'atmophile', highly volatile nature of the noble gases make them useful tracers of a range of geological processes, from Earth's atmospheric evolution to the preservation of deep mantle heterogeneity. Coupled with the range of long-lived and extinct parent radionuclides that lead to noble gas daughter products, the noble gases offer one of the most exceptional geochemical 'element suites' for understanding volatiles, and the evolution of Earth's ocean and atmosphere (e.g., Moreira, 2013; Marty, 2020).

In addition to volatile studies at Earth's surface, the noble gases have been instrumental in providing geochemical insight to Earth's interior structure. Discovery of helium-3 emanating from well gases (Alvarez & Cornog, 1939; Aldrich & Nier, 1946; Mamyrin et al., 1969), and as excesses in seawater (Clarke et al., 1969), paved the way for the interpretation of this signal as representing trapped primordial gases in Earth's mantle implanted into the planet during accretion. During the late 1960s and early 1970s it was increasingly recognized that ocean island basalts (OIB) were distinct in their trace element geochemistry and in their long-lived radiogenic isotope compositions compared with mid-ocean ridge basalts (e.g., Gast et al., 1964; Engel et al., 1965). Focus on helium (Kaneoka & Takaoka, 1980; Kurz et al., 1982), xenon (Hennecke & Manuel, 1975; Kaneoka & Takaoka, 1980), argon (Fisher, 1983), and finally neon isotopes (Sarda et al., 1988; Honda et al., 1991), led to observations of low $^{4}He/^{3}He$ and excesses of $^{20}Ne/^{22}Ne$, $^{40}Ar/^{36}Ar$ and xenon isotopes relative to the atmosphere. The other noble gases, radon and krypton, have not been considered much in OIB studies, due to the radiogenic nature of the former, and the difficulty in analyzing the latter.

Since the initial pioneering studies on noble gases in OIB, there has been proliferation in He isotope analyses as well as progressive improvements and an increase in available data for Ne, Ar and Xe isotopes. In particular, helium isotopes in OIB, which are often expressed as $^{3}He/^{4}He$ ratios relative to the air value ($R/R_A = 1/(^{4}He/^{3}He \times \text{air } [0.000001384])$, have been highly influential in scholarly discourse surrounding OIB petrogenesis, from geochemical studies (e.g., Kurz et al., 1982), to understanding mantle structure from seismic tomography (e.g., Williams et

al., 2019), to geodynamic modelling of mantle interior structure (e.g., Van Keken & Ballentine, 1998; Xie & Tackley, 2004), or to the perspective of hot, deep mantle plumes (e.g., Jackson et al., 2017). The high-$^3He/^4He$ component in OIB has attracted significant attention, being interpreted as a signature of a deep mantle source and, most recently, as a relatively pristine mantle source. Relatively pristine mantle sources with high-$^3He/^4He$ have been variably described as the lower mantle-derived focus or focal zone (FOZO), which is ancient and depleted (Hart et al., 1992; Jackson et al., 2020), or the primitive He mantle (PHEM), interpreted to be primordial with near bulk silicate earth Sr and Nd isotopic compositions (Farley et al., 1992). An alternative component which can have high-$^3He/^4He$ has also been proposed, called the common or C component, which likely contains subducted oceanic crust, is not primordial or pristine and is located either in the mantle transition zone or at the core mantle boundary (Hanan & Graham, 1996). The currently most popular component discussed is FOZO, as the C component requires mixing and diffusion of primordial noble gases to explain high-$^3He/^4He$ in some locations. In many cases, studies assume the maximum He isotope compositions are representative of OIB and use these to compare with geophysical parameters (e.g., Jackson et al., 2017; Williams et al., 2019). Studies of the other noble gases have revealed evidence for solar components in OIB, albeit attempts to link these noble gases in combination have been relatively limited. The studies that have done this have provided important insights into OIB petrogenesis (see for example, Moreira, 2013; Parai et al., 2019 and Mukhopadhyay & Parai, 2019).

Following from studies of noble gases in combination, the goal of this work is to consider and synthesize the currently available noble gas isotope data for OIB. Particular attention is given to the type of samples used to obtain noble gas isotope data on OIB, potential processes that might affect noble gas isotopes in these samples, and to investigate the fidelity of using maximum He isotope ratios associated with a given OIB chain. Evidence from He-Ne-Ar-Xe isotope systematics is paired with extinct and long-lived radiogenic isotopes (Sr-Nd-Os-W-Pb) to explore the likely sources of OIB, and to consider the probable nature of the mantle in terms of both structure and composition.

2. On the measurement of noble gases in OIB

The measurement of noble gas isotopes has continued to advance since initial discovery of ^3He in natural gas samples in the late 1930s and early 1940s (Alvarez & Cornog, 1939; Aldrich &

Nier, 1946) and, specifically, emanating from mantle samples in 1969 (Clarke et al., 1969; Mamyrin et al., 1969) and from trapped inclusions within OIB mineral grains in 1980 (Kaneoka & Takaoka, 1980). Despite the advantages of measuring noble gases in mantle samples due to their generally inert chemical behaviors, the low abundances of He, Ne, Ar, Kr and Xe in terrestrial volcanic rocks and their mineral components makes determination of their abundances and isotopic compositions challenging. In particular, the abundances measured in even some of the most gas-rich volcanic samples by crushing them (cf., the 'popping rock' 2ΠD43; He = ~2.9 ppmv; Ne = ~0.008 ppbv; Ar = 1 ppmv; Xe = 0.0001 ppbv; Parai & Mukhopadhyay, 2021) are, in some cases, far lower than their abundances within Earth's atmosphere (He = 5.24 ppmv; Ne = 18 ppmv; Ar = 9340 ppmv, Kr = 1.1 ppmv; Xe =0.087 ppmv; **Table 1**). All noble gases are therefore susceptible to air contamination prior to, or during sampling, or due to contamination during laboratory analyses. As discussed later, the noble gas most minimally affected by recycling of atmospheric noble gases into the deep Earth is He, which is lost from the atmosphere to space, with a mean residence time of ~1 million years (Farley & Neroda, 1998; Marty, 2020). For these reasons, studies of He isotopes in OIB are plentiful, whereas studies of Ne, Ar or Xe are more limited, with studies of Kr isotopes being virtually absent.

When discussing noble gases in OIB, it is critical to assess the sample media from which they were measured (e.g., glasses, minerals, geothermal gases or fluids), with this media being important for four principal reasons. Firstly, due to their extreme incompatibilities and similar behavior with respect to solubility, diffusivity, and crystal-melt partitioning, the noble gases partition preferentially into silicate melts during partial melting, and then into fluid (H_2O) or gas phases (CO_2-rich) during further magmatic exsolution. Secondly, solubilities of the noble gases reverse between silicate liquids, where He is most soluble and Xe is least soluble, to water, where Xe is most soluble and He is least (e.g., Ozima & Podosek, 2002; Mukhopadhyay & Parai, 2019). Due to these properties, the potential to trap heavier noble gases within subducted seawater components makes them useful for understanding recycling into the deep mantle (Holland & Ballentine 2006, Kendrick et al. 2011; 2018). A third aspect of the sample media type is that the noble gases can be trapped, accidentally, within fluid or melt inclusions in minerals, within fast-quenched glasses, and can emanate from volcanic edifices trapped within fluids or in the gas phase. Magmas or hydrothermal fluids and gases erupted under higher confining pressures, for example beneath water or ice, will retain higher intrinsic noble gas contents than those erupted subaerially,

simply expressed by the Ideal Gas law (PV = nRT, where P is pressure in pascals, V is volume in cubic meters, n is the amount of the gas in kg, R is the ideal gas constant of 8.3145 J K^{-1} mol^{-1} and T is temperature in kelvin). This means that 'pristine' mantle-derived noble gas samples are exceptionally rare.

Fourth is the susceptibility of the media to secondary alteration processes. For example, geothermal fluids and gases need to be trapped at the time of emanation from their source and so represent ephemeral media for examining noble gas compositions. Glasses tend to slowly crystallize after they have cooled and, although some ancient glasses can be preserved, the relatively elevated K, U and Th contents within them can result in significant production of radiogenic noble gas contents. In the case of mineral grains that form early within magmas (olivine and clinopyroxene), they can preserve mantle He isotopic compositions for more than 100 million years (e.g., Basu et al., 1995; Stronik et al., 2017), but are also susceptible to ingrowth of radiogenic noble gases, and the effectiveness of trapping noble gases within minerals is generally poor (Horton et al., 2019).

The above-mentioned aspects of noble gas behavior make estimating their abundances in both parental melts and their mantle sources difficult. Examination of noble gases in OIB is therefore quite different from that for stable or radiogenic isotope systems, where elemental concentrations are more readily quantified. As discussed later, combination of these systems can be both powerful but may also be misleading. The behaviors of noble gases during partial melting, eruption and post-emplacement means that mixing between atmospheric and mantle noble gas components are likely to increase with decreasing confining pressures of magmas or exsolved gases. The consequence of these behaviors is that a popular method is to extrapolate to mantle compositions, free from recent atmospheric contamination, especially for Ne, Ar and Xe isotopes (e.g., Mukhopadhyay & Parai, 2019).

Despite the different behaviors of geothermal fluids and gases versus glasses or minerals, the comparison of their isotopic compositions is especially useful in modern OIB settings where both media can be found. Helium is by far the best sampled of the noble gases, so the temporal and spatial distributions of noble gases evident in OIB have to be extrapolated from the atomically lightest amongst them. Nowhere are temporal and spatial variations in noble gases better expressed than in Iceland, where the bedrock geology is, for the most part, relatively recently erupted basaltic rock and where geothermal springs and fumaroles are plentiful. Taking advantage of over 800

measurements of noble gases in various Icelandic sample media, Hardardottir et al. (2018) provided a comprehensive assessment of helium isotopic variations, demonstrating a wide range in $^{3}He/^{4}He$ (5.1 to 47.5 R_A) and denotating systematic variations between individual rift segments and off-rift regions. They showed that an average high-$^{3}He/^{4}He$ component decreases from the Eastern (18-21 R_A) to the Western (12-17 R_A) to the Northern Rift Zone (8-11 R_A) placing the center of the high-$^{3}He/^{4}He$ plateau towards southwest Iceland. The study of Hardardottir et al. (2018) highlights both the spatial variability of noble gas compositions within active volcanic regions, but also provides a temporal link, showing that Miocene-aged volcanic rocks of NW Iceland have the highest-$^{3}He/^{4}He$ (e.g., Hilton et al., 1999).

To examine temporal and spatial variations in noble gases within OIB, Day & Hilton (2021) undertook a wider survey of helium isotope compositions preserved in geothermal fluids and gases compared to minerals or glasses. Using examples from the Canary Islands, Azores, Cape Verde, Hawaii and Iceland they showed generally good correspondence between different sample media from the same locations, even across >1 Ma of stratigraphy (**Figure 1a**). Nonetheless, they also recognized examples of inter-island heterogeneity in He isotopes at Hawaii, the Azores, and within Iceland preserved in both hydrothermal samples, minerals and glasses. Day & Hilton (2021) pointed out that in northwest Iceland, olivine separates from older lavas preserve higher-$^{3}He/^{4}He$ than present-day geothermal samples from the same region reflecting a reduced mantle-derived ^{3}He input to Icelandic magmatism since the Miocene, emphasizing changing distributions in noble gases both temporally and spatially within OIB. Directly mapping the geothermal gases and fluids emanating in NW Iceland, with minerals trapped within more ancient lavas poses a similar issue to comparing seismic images of the deep mantle with ancient lava compositions, and such direct comparisons are not warranted unless temporal variations are taken into consideration.

Even within solid samples noble gas compositions can be radically different. Studies of OIB noble gas isotopes can use both minerals and glass, and distinct He isotopic compositions have been measured between olivine and glass in Icelandic lavas (e.g., ~9 R_A in glass and 6 R_A in olivine from sample NAL 688; Macpherson et al., 2005). Significant differences between olivine and clinopyroxene within the same lavas from a range of OIB localities have also been found (**Figure 1b**). Helium isotope ratios measured in these minerals demonstrate that olivine will always have the same or higher $^{3}He/^{4}He$ than the co-existing clinopyroxene, indicating that it is a more

faithful recorder of He isotope composition, while absolute gas contents vary non-systematically by an order of magnitude between the two media (Day & Hilton, 2011).

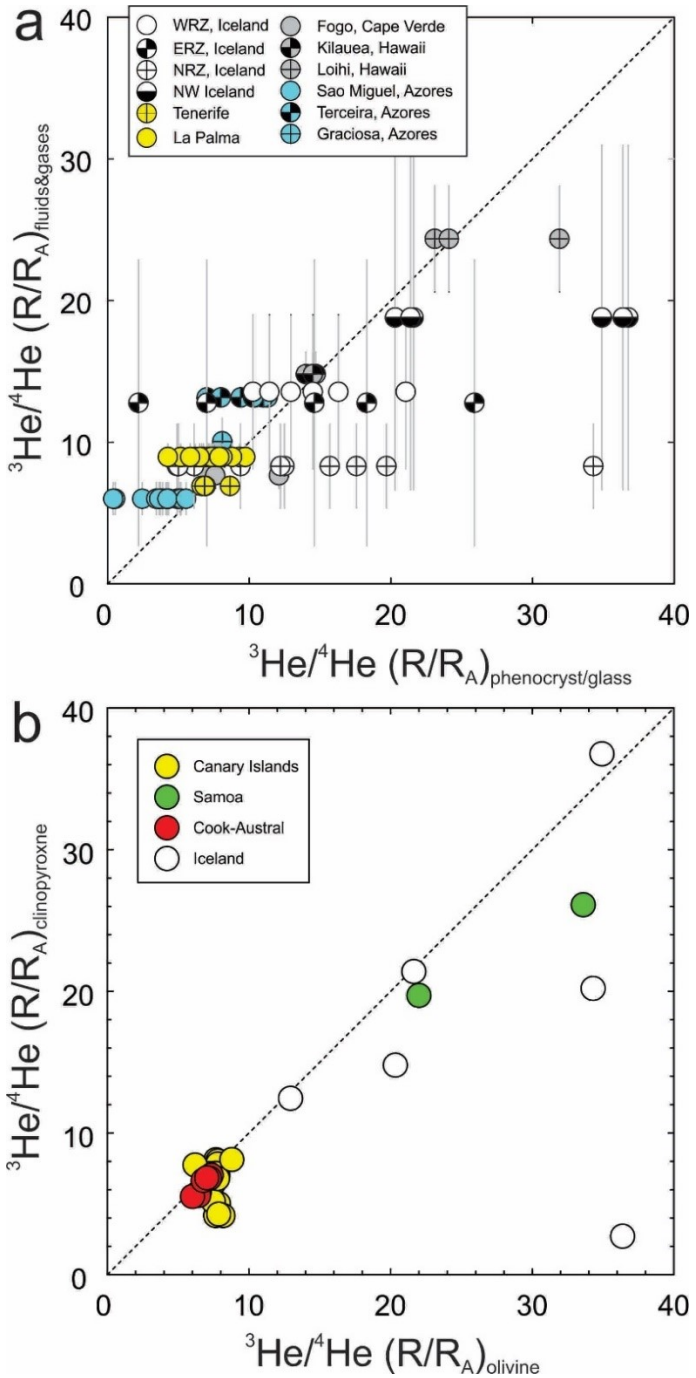

Figure 1: *(a) Measured (a) $^3He/^4He$ (R/R_A) ratios for paired olivine and clinopyroxene separates from the Canary Islands (Day & Hilton, 2011), Samoa (Jackson et al., 2007), the Cook-Austral Islands (Hanyu et al., 2011) and for Iceland (Macpherson et al., 2005; Füri et al., 2010). (b) Helium isotope variations for phenocrysts (olivine, pyroxene) and glass versus hydrothermal samples from the same locations. Data for the Canary Islands are from Day & Hilton (2011; 2021) and Gurenko et al. (2006). Data for the: Azores are from Moreira et al. (1999; 2012) and Jean-*

Baptiste et al. (2009); Hawaii are from Kurz et al. (1982), Sedwick et al. (1994) and Hilton et al. (1997); Iceland are from Macpherson et al. (2005) and Füri et al (2010).

A final complication when measuring noble gases in OIB relates to the release of cosmogenically and radiogenically produced species during analyses. For example, both cosmogenic thermal-neutron generation of ^{3}He and radiogenic ingrowth of ^{4}He by alpha decay of U and Th can modify He isotope compositions in rocks over time. In a compilation of He isotope results from both crushing and melting experiments performed on olivine and pyroxene grains, Day et al. (2015) showed greater dispersion in ^{3}He/^{4}He for melting experiments through the liberation of both ^{3}He generated by cosmogenic spallation and/or thermal neutron capture, and ^{4}He from radioactive decay of U and Th. These results support experiments that adopt a step-wise crushing approach, where samples were repeatedly crushed for fixed but limited durations without breaking vacuum, leading to consistency of ^{3}He/^{4}He and indicating restricted contributions from matrix gas (Hilton et al., 1993; 2011; Scarsi, 2000; Blard & Farley, 2008). On the other hand, crushing may not release all magmatic volatiles and the specific population of crystals measured may lead to significant variations in noble gas content (e.g., Horton et al., 2019).

The examples described above relate to helium, rather than directly to Ne, Ar, Kr or Xe which all have lower inherent gas contents making them harder to measure, particularly in magmatic minerals, while mixing with atmosphere make it difficult to measure mantle isotopic signatures of the heavier noble gases in hydrothermal gases or fluids. Instead, the majority of measurements of Ar and Xe in particular have either been conducted by crushing or melting of glasses erupted at high confining pressures, or using deeply derived cumulate mineral grains (e.g., Trieloff et al., 2000). These differences in noble gas behavior and abundance, both in space and time, place restrictions on available noble gas isotope data for OIB, but also provide information on magmatic process and noble gas preservation, as discussed below.

3. Complications of degassing and partial melting

Radiogenic isotope systems (e.g., Sr, Nd, Hf, Os, Pb, W) measured in OIB are largely unaffected by crustal assimilation, except if they are in extremely low abundance. The reason for this is that the edifice into which they are erupted is often similar in composition to the magmas themselves and are young; no older than the oceanic plate on which they reside, less than 200 million years. This is not the case for noble gases. Due to variable gas contents, some OIB samples

can have noble gas isotope compositions that trend to that of the atmosphere due to concomitant degassing and assimilation processes (e.g., Hilton et al., 1995). Again, helium is the best studied of the noble gases in OIB, and a diagram of ^{4}He content [He] versus measured ^{3}He/^{4}He, largely measured in olivine mineral separates illustrates this issue (**Figure 2**).

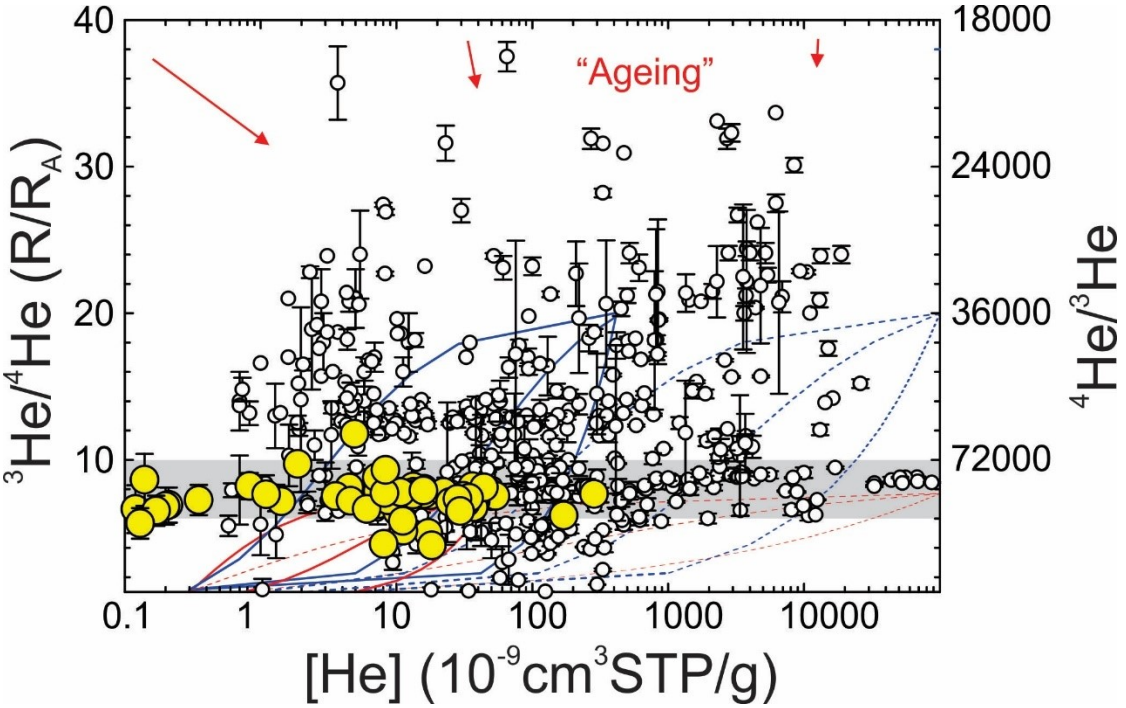

Figure 2: *Helium concentrations versus ^{3}He/^{4}He for olivine and clinopyroxene separates from a global suite of OIB, with example of a single OIB chain (Canary Island lavas as yellow circles; Day & Hilton, 2011). The effect of variable degassing and contamination on helium within mineral separates is shown assuming mixing between a possible parental magma He composition (here inferred to be helium in parental melts of various abundances and with between 20 to 8 R_A, with a degassed and aged (0.1 Ma) edifice basalt composition with 1 ppm U and Th/U = 4 and initial ^{3}He/^{4}He = 8 R_A (present day ^{3}He/^{4}He = ~0.3R_A, [He] = 0.25 ×10^{-9} cm^{3}stp/g). The ratio of helium concentration in the melt relative to the assimilant is shown as no degassing of parental magma (ratio = 1), order of magnitude gas loss (0.1), and two orders of magnitude gas loss (0.01). Arrows denote the effect of 'ageing' of ^{3}He/(U+Th) in phenocrysts. Ageing will affect low [He] content melts more than higher [He] content equivalents, illustrated by the size and orientation of vectors. Field of canonical mid-ocean ridge basalt (MORB; 8 ± 2 R_A; Graham, 2002) is shown as a gray bar, for comparison.*

Aside from the issues of efficient gas release during crushing, data in **figure 2** reveal over six orders of magnitude variation in He abundance, with OIB samples with MORB-like ^{3}He/^{4}He spanning all of this variation and OIB with >30 R_A showing at least three orders of magnitude variation. Previous efforts to model degassing with concomitant assimilation of radiogenic He

demonstrates that for addition of radiogenic He to have noticeable effects, there must be in excess of an order of magnitude gas loss from presumed parental melt gas abundances, meaning that accurate noble gas systematics depend upon severely limiting crustal assimilation contributions to less than 1% (Day & Hilton, 2011). Similarly, work to establish variations of noble gas compositions in OIB through ageing of magmas and the generation of ^{4}He through radiogenic decay of U and Th have been proposed (e.g., Moreira & Allegre, 2004), but are generally considered to play a limited role, both within minerals as well as in geothermal fluids and gases unless total He abundances are exceptionally low (e.g., Day & Hilton, 2011; 2021; Truong et al., 2018).

The near-perfectly incompatible behavior of noble gases during mantle partial melting could lead to the assumption, in some instances, that the noble gas isotope compositions of lavas are a faithful reflection of their bulk mantle source. This assumption differs from other isotopic variations within OIB which are normally attributed to partial melting of distinct mantle components (e.g., Zindler & Hart, 1986; Hofmann 1997; Brandon et al., 2007; Day et al., 2009). The degree of partial melting, however, may have a profound effect on OIB noble gases. Melting of more fusible components in the mantle source, over those that are more refractory, will affect the noble gas composition of the erupted lavas during preferential gas-release. In turn, lower degree partial melts will sample more diminutive noble gas components versus higher degree partial melts, and the solubilities of noble gases in silicate melts will also affect this outcome. This issue will be returned to in later sections, but one such example is offered by using simple estimates of island volume versus the He isotope compositions measured on islands. It is possible to provide crude volume estimates for volcanic islands, from the surrounding mean water depths and their height. From these estimates and eruption ages, mean melt flux estimates can also be deduced. In the case of the Samoan Islands, the broadly age progressive nature of the islands (Hart et al., 2004) means that their estimated volumes can be used as a proxy of total melt volumes that reached the surface. From detailed study, it has been recognized that He isotope compositions vary within the islands, from nearly MORB-like ^{3}He/^{4}He, to high-^{3}He/^{4}He (e.g., Jackson et al., 2007; 2014). If the measured He isotope composition in surface samples reflects the overall volcanic edifice, then there is a relationship with the highest-^{3}He/^{4}He being measured in volcanoes with small total island volumes (**Figure 3**). Such an analysis is by no means perfect, since it has been established that He isotope variations can occur temporally within a single island's lava stratigraphy (Kurz et al.,

316 1996), but it nonetheless illustrates that the degree of partial melting is likely to play a role in
317 determining noble gas isotopic compositions.

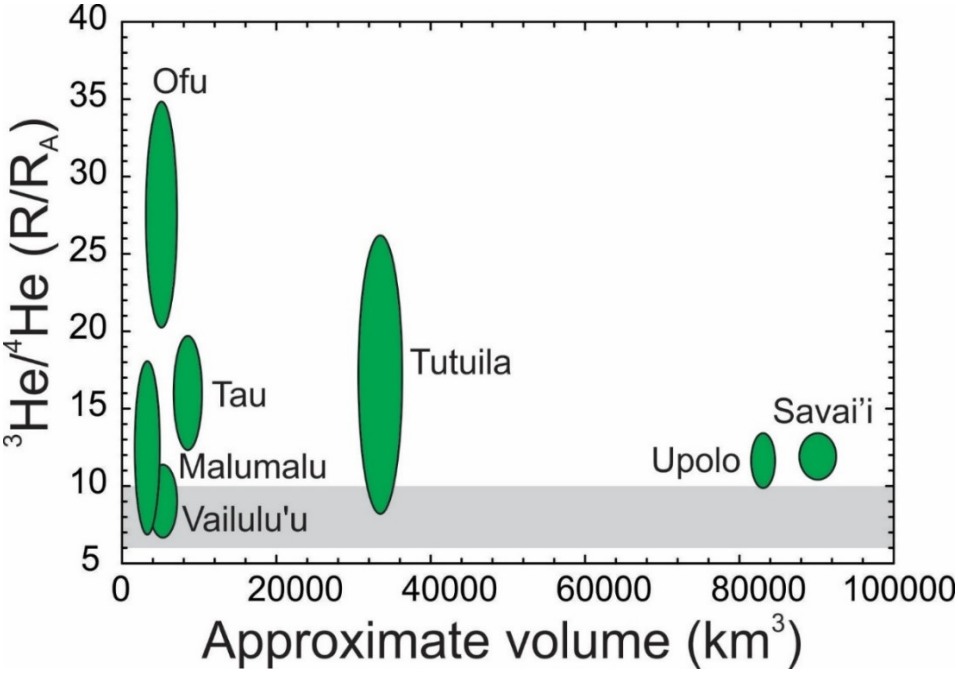

318

319 ***Figure 3:*** *Approximate edifice volume (in km^3) versus range in helium isotope compositions for*
320 *some of Samoan Islands and seamounts. Volume estimate taken from analysis of volcano depth,*
321 *radius and height using maps of the islands, and He isotope compositions are from Jackson et al.*
322 *(2014) and references therein. Shapes of ellipses denote approximate uncertainties in volume and*
323 *He isotope composition.*
324

325 **4. Using helium isotopes to determine OIB mantle sources**

326 It is seemingly no exaggeration that every major ocean island in the world with sub-aerially
327 exposed volcanic rock has a helium isotope measurement of one type or another reported in the
328 literature for it. For some islands, like Iceland, the range of He isotope compositions is significant
329 (5.1 to 47.5 R$_A$), demonstrating that within individual islands, He isotope variations can be
330 significant, as also has been observed in Samoa (e.g., **Figure 3**). Most studies have used mineral
331 grains (olivine, clinopyroxene) to obtain these results, although glasses are sometimes also
332 available, and these data are the main stay of OIB He isotope studies.

333 For various reasons, He isotope studies considering global OIB typically take the approach
334 of taking the maximum He isotope compositions and grouping island chains under this value (e.g.,
335 Jackson et al., 2017; Williams et al., 2019). This approach has both strengths and weaknesses, as

the variability in He isotope compositions may reveal much about magmatic processes. Nonetheless, taking this same approach, OIB can be broken into four basic categories (**Table 2**).

1. Low-$^3He/^4He$ OIB (<7 R_A; $^4He/^3He$ = >110,000): A restricted group of OIB with $^3He/^4He$ ratios at or below the MORB range (8 ±2 R_A; Graham, 2002), termed low-$^3He/^4He$ OIB include a few individual islands, such as São Miguel in the Azores (Moriera et al., 2012), as well as Saint Helena (Hanyu et al., 2011), Mangaia (Parai et al., 2009), Grande Comore Island (Class et al., 2005), and Guadalupe Island (Eiler et al., 1997).
2. MORB-like $^3He/^4He$ OIB (8 ±2 R_A; $^4He/^3He$ = 110,000 to 70,000): A more common type with MORB-like $^3He/^4He$, including Ascension Island (Ammon et al., 2009), Balleny Island (Williams et al., 2019), the Canary Islands (Hilton et al., 2000; Day & Hilton, 2011), the Cobb Islands (Lupton et al., 1993), the Comoros (Class et al., 2005), Mount Erebus (Day et al., 2019), Gough and Tristan da Cuhna (Class et al., 2005), Madeira (Vance et al., 1989), Marion and Prince Edward Islands (Williams et al., 2019), Rodrigues (Furi et al., 2011) and Socorro Island (Taran et al., 2002).
3. An intermediate-$^3He/^4He$ OIB group (10-~20 R_A; $^4He/^3He$ = <70,000 to ~35,000): Using the simple approach of lumping islands under their highest $^3He/^4He$, this would be the largest group, including the Azores (although see 1.; Madureira et al., 2005), Bouvet (Kurz et al., 1998), Cape Verde (Doucelance et al., 2003), Caroline Islands (Jackson et al., 2017b), Discovery seamounts (Sarda et al., 2000), Easter Island (Poreda et al., 1993), Heard Island (Hilton et al., 1995), Juan Fernandez Islands (Farley et al., 1993), Louisville seamounts (Hanyu, 2014), Macdonald and the Cook Australs and Macdonald Seamount Chain (although see 1.; Moreira and Allegre, 2004), the Marquesas (Castillo et al., 2007), Mauritius (Furi et al., 2011), the Meteor hotspot and Shona Island (Moriera et al., 2005), Pitcairn Island (Garapic et al., 2015), Reunion Island (Staudacher et al., 1990; Furi et al., 2011), Tahiti and the Society Islands (Hanyu et al., 1999), Crozet Island (Breton et al., 2013) and Amsterdam and St. Paul (Graham et al., 1999).
4. High-$^3He/^4He$ OIB group (>25 R_A; $^4He/^3He$ = <30,000): Representing the *crème-de-la-crème* of OIB for helium, these are Iceland (Hilton et al., 1999), Hawaii (Valbracht et al., 1997), the Galapagos (Kurz et al., 2009) and Samoa (Jackson et al., 2009). Some studies include the Palaeogene Baffin Island and West Greenland picrites, which can have high-$^3He/^4He$ (up to 50R_A; e.g., Stuart et al., 2003) within this OIB grouping. These picrites are continental flood

basalts, forming part of the North Atlantic Igneous Province, and are susceptible to crustal contamination effects (Day, 2016), hence – so not to 'muddy the water' - we elect not to include them in this assessment.

As noted above, the waters are far murkier than this simple evaluation might suggest. This is illustrated by noting the range within the Samoan Island chain (**Figure 3**), and cross-island chain studies illustrate significant helium isotope variability (e.g., Kurz et al., 1996; 2009; Class et al., 2005; Macpherson et al., 2005; Madureira et al., 2005). Ignoring He isotope variability in OIB may be important for assessing whether He is truly derived from the hottest mantle plumes (e.g., Jackson et al., 2017), or if it is sourced from seismically slow regions of the lower mantle (Williams et al., 2019). Significantly, it avoids the question of chemical heterogeneity, a variable that is key to understanding the mantle's mixing history and the origin of primitive components; topics we now return to.

A method that has provided important information on mantle isotopic variability has been to compare helium isotope variations with radiogenic isotopes. An example of He isotope data versus radiogenic isotopes is shown in **Figure 4**, where He isotope measurements dominantly from olivine grains have been compared with bulk rock $^{143}Nd/^{144}Nd$ and $^{206}Pb/^{204}Pb$ data. Much has been written about the relationships in **Figure 4** in the references cited relating to He isotope compositions in OIB, listed above, and will not be repeated in detail here. The basic premise is that low-$^{3}He/^{3}He$ and MORB-like $^{3}He/^{4}He$ OIB groups span a wide range of Sr-Nd-Pb isotope compositions, spanning from HIMU-like (high $^{206}Pb/^{204}Pb$), to having depleted MORB mantle (DMM, high $^{143}Nd/^{144}Nd$), to enriched mantle flavors (low $^{143}Nd/^{144}Nd$, high $^{87}Sr/^{86}Sr$). Conversely intermediate-$^{3}He/^{4}He$ to high-$^{3}He/^{4}He$ OIB typically span more restricted ranges in Sr-Nd-Pb isotopes, and possibly encapsulate two distinct high-$^{3}He/^{4}He$ reservoirs (Jackson et al., 2007). The wide range in Sr-Nd-Pb isotopes for the low- and MORB-like $^{3}He/^{4}He$ OIB has typically been explained through recycling of subducted crustal components and variable mixing with DMM.

Conversely, the intermediate- and high-$^{3}He/^{4}He$ OIB have been considered to come from a common reservoir, variably termed in the literature as the 'C' or common component (Hanan & Graham, 1996), 'PHEM' of Primary Helium Mantle (Farley et al., 1992), and most commonly 'FOZO', or the Focal Zone (Hart et al., 1992), now more commonly referred to as the Focus Zone. As mentioned previously, these are slightly different flavors of the same theme, with the

interpretation that the elevated ^{3}He component comes from the deep mantle. Debate continues as to what the nature of the deep mantle component might be, from early mantle domain(s) that dominates the isotopic character of resultant lavas (e.g., Class et al., 2005; Jackson et al., 2010; 2020) to mixed sources of subducted components and relatively less degassed lower mantle (e.g., Gonnerman & Mukhopadhyay, 2009).

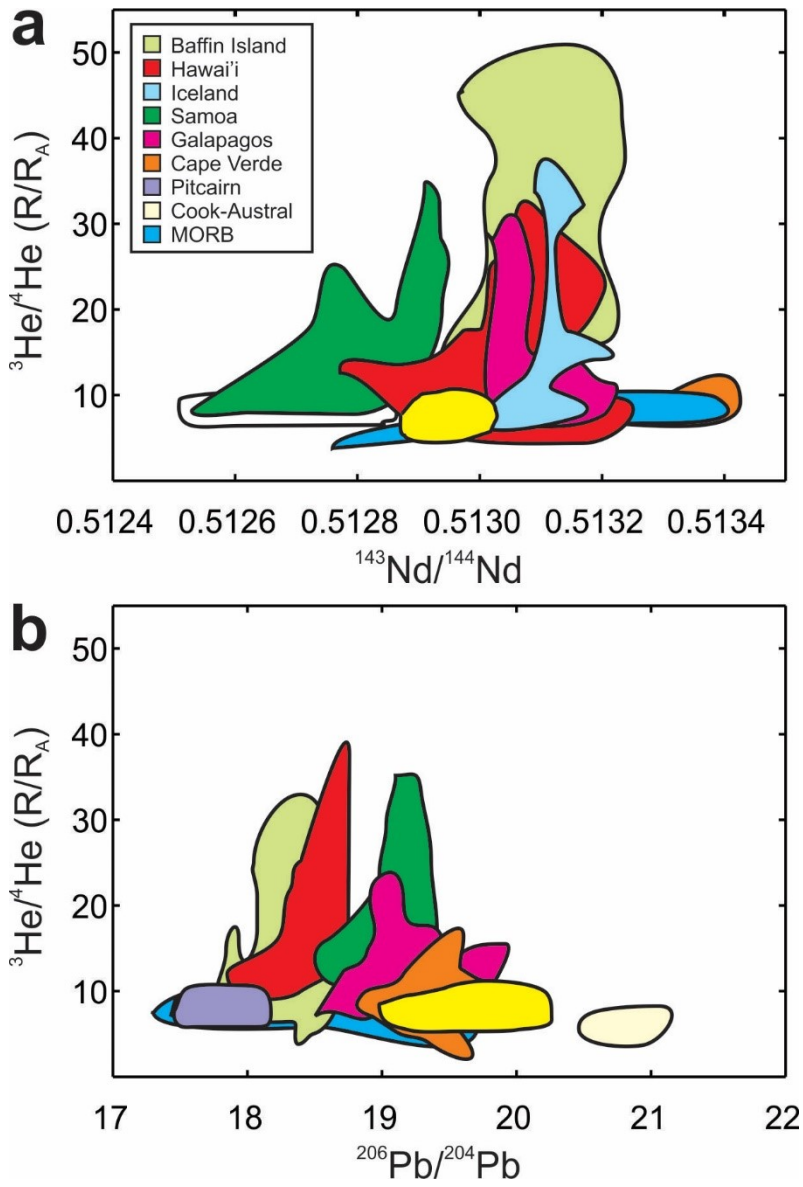

Figure 4: *$^{3}He/^{4}He$ from olivine separates versus (a) $^{143}Nd/^{144}Nd$ and (b) $^{206}Pb/^{204}Pb$) shown as fields. Figure modified from Day & Hilton (2011). The yellow field is the Canary Islands shown in prior figures.*

A new line of evidence is the relationship between high-$^{3}He/^{4}He$ and $^{182}W/^{184}W$. Tungsten-182 is the decay product of ^{182}Hf, which had a half-life of 9 million years. Consequently, variations measured in $^{182}W/^{184}W$ for OIB reflect heterogeneities imparted within the first 60 million years or so of Earth's history, and such variations have recently been detected, with notable differences in $^{182}W/^{183}W$ between low- and MORB-like $^{3}He/^{4}He$ OIB and lavas with high-$^{3}He/^{4}He$ (Mundl et al., 2017). This original paper noted a correlation between He and W (**Figure 5**) interpreted to support a deep mantle plume origin (Mundl et al., 2017), possibly even from the core-mantle boundary (Mundl-Petermeier et a., 2020), and for ancient heterogeneities to be preserved, intact, within the lower mantle (Jackson et al., 2020).

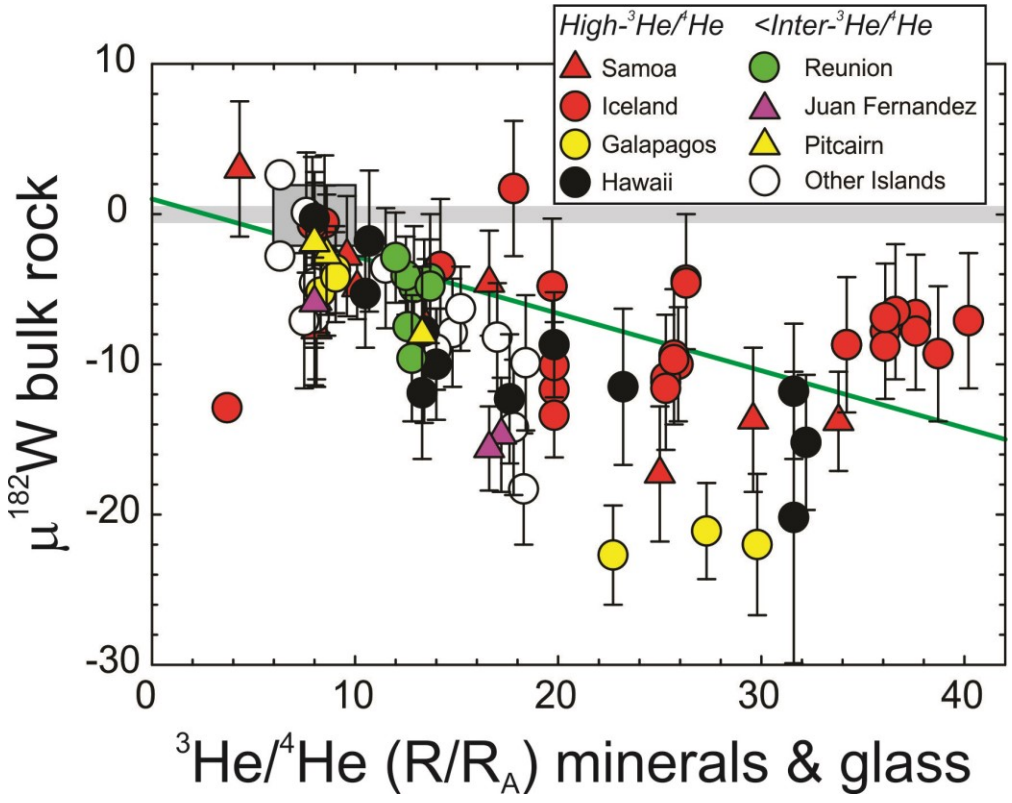

Figure 5: *Helium versus tungsten isotopes in OIB. The original correlation line from Mundl et al. (2017) is shown in green, with the terrestrial standard shown as a grey line and the DMM value shown as a grey box, assumed using the average MORB $^{3}He/^{4}He$ ratio from Graham (2002). Tungsten isotope data are from Mundl et al. (2017), Mundl-Petermeier et al. (2019, 2020), and Peters et al. (2021), with He isotope data sources reported in those works.*

Since 2017, the available high-precision $^{182}W/^{184}W$ data for OIB have increased substantially and the correlation is not as strong (**Figure 5**). In general, high-$^{3}He/^{4}He$ OIB are always lower than the terrestrial standard for W isotopic composition (reported in ppm deviations, or $\mu^{182}W$), suggesting derivation from low-Hf/W reservoirs, such as the core, or from anomalous regions of the lower mantle. Arguments have been made to explain individual correlations between He and W (Mundl-Petermeier et al., 2019; Jackson et al., 2020), although these arguments rely on an assumed reservoir concentration for both noble gases (He) and tungsten.

An example of contrasting interpretation of different trends comes from He-W isotope correlations for Icelandic lavas. Mundl-Petermeier et al. (2019) reported two groups of lavas; a 'Low-Pb' group, consisting mostly of basalts from NW Iceland with $^{206}Pb/^{204}Pb$ from ~18.4 to 18.5, $^{3}He/^{4}He$ from 17.8 to 40.2R_A, and $\mu^{182}W$ from +1.7 to −9.1 and; a 'High-Pb' group, consisting mainly of recent basalts, with higher $^{206}Pb/^{204}Pb$ (~18.7 to 19.2), $^{3}He/^{4}He$ from 7.9 to 25.7R_A, and $\mu^{182}W$ from −0.6 to −11.7 (**Figure 6a**). These authors explained the variations as mixing between ambient upper oceanic mantle and primordial reservoirs that underwent limited de-gassing, one of which formed within the first 60 Ma of Solar System history and was a major contributor to the youngest basalts.

In this interpretation, there remain some important research questions. For example, the 'low-Pb' trend is dominated by Miocene samples from NW Iceland, yet one recent basalt (ICE-14-32A) is in this grouping. Similarly, one Miocene sample (ICE-14-16) is excluded due to slightly more radiogenic $^{206}Pb/^{204}Pb$. Also not well understood is the relationship of He-W isotope compositions and [He] contents (**Figure 6b**). In the recent 'high-Pb' lavas, there is a trend of decreasing $^{3}He/^{4}He$ with decreasing [He], that broadly correlates with W isotope anomaly. This would be consistent with low-$^{3}He/^{4}He$ lavas having greater contributions from a crustal or upper mantle source with concomitant degassing and assimilation. On the other hand, the 'low-$^{3}He/^{4}He$' NW Iceland samples show no trend, but the samples with the highest [He] contents also have the lowest $^{3}He/^{4}He$ and $\mu^{182}W$. As noted from geothermal fluid and gas versus phenocryst and glass comparisons (Hardardottir et al., 2018; Day & Hilton, 2021), the high-$^{3}He/^{4}He$ component in earlier Icelandic lavas are not readily sampled in modern Icelandic rift lavas, and it is possible that the He-W isotope compositions and [He] contents indicate temporal variations in isotopic signatures flavored from pulsing of deep plumes.

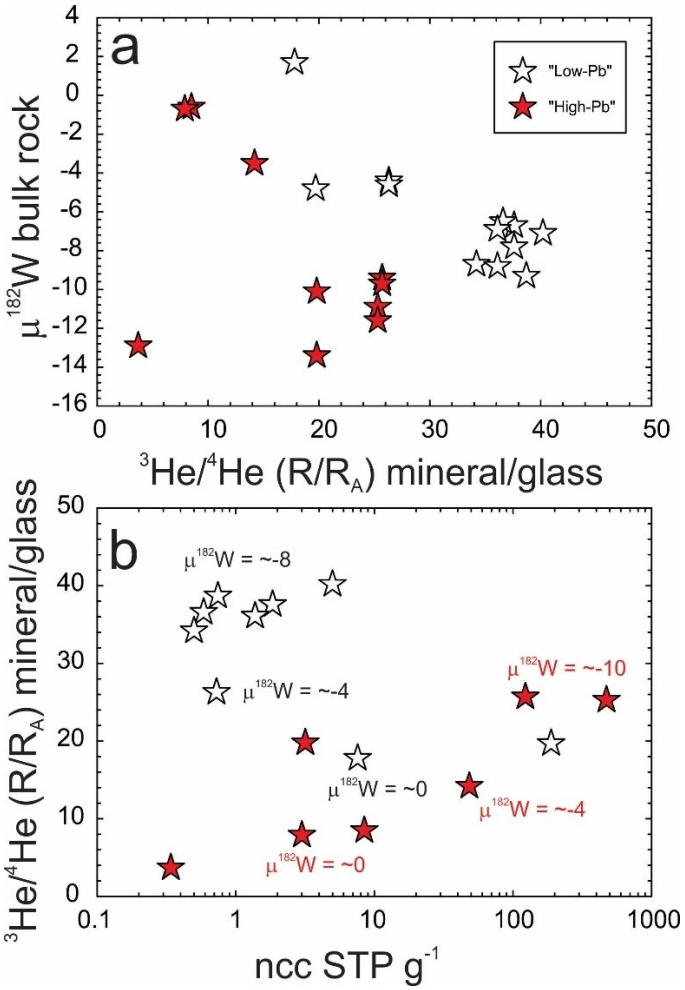

Figure 6: (a) *Helium-W isotope and (b) Helium isotope and abundance data for 'low-Pb' and 'high-Pb' Icelandic lava data from Mundl-Petermeier et al. (2019), with W anomalies shown beside groupings. See text for details.*

Trends between helium isotopes and radiogenic isotopes are not restricted to Sr-Nd-Hf-Pb or extinct radionuclides, but occur with highly siderophile elements, like Os. Brandon et al. (2007) in their study of Icelandic rift zone lavas noted positive correlations with $^{187}Os/^{188}Os$ and $^{3}He/^{4}He$, similar to correlations for Hawaiian volcanoes (Brandon et al., 1999). These have been interpreted to reflect mixing between high-$^{3}He/^{4}He$ deep mantle components, possibly including the core, and upper mantle products, or depleted components within the mantle plume beneath Iceland (**Figure 7**). In these Icelandic lavas, there is a relationship between the lowest $^{3}He/^{4}He$ samples having the most depleted Nd, Hf and Pb isotope compositions and the more enriched lavas having high-$^{3}He/^{4}He$ (Nicklas et al., 2021). A broader comparison of He-Os isotope data for several OIB chains suggests a slightly different picture, where OIB with radiogenic $^{187}Os/^{188}Os$ generally have

$^{3}He/^{4}He$ within the MORB-range, whereas high- and intermediate-$^{3}He/^{4}He$ OIB have $^{187}Os/^{188}Os$ close to primitive mantle estimates (~0.1296; Meisel et al., 1996). As with He-W and some He-Sr-Nd-Pb isotope systematics, this suggests different processes, including the extent of partial melting and the contribution from different mantle reservoirs, playing a role in the ultimate isotopic composition of lavas. Similar evidence lies in measurement of oxygen isotopes with He isotopes in the same olivine populations, suggesting distinct mantle lithologies being sampled in some OIB (Day et al., 2009; 2010).

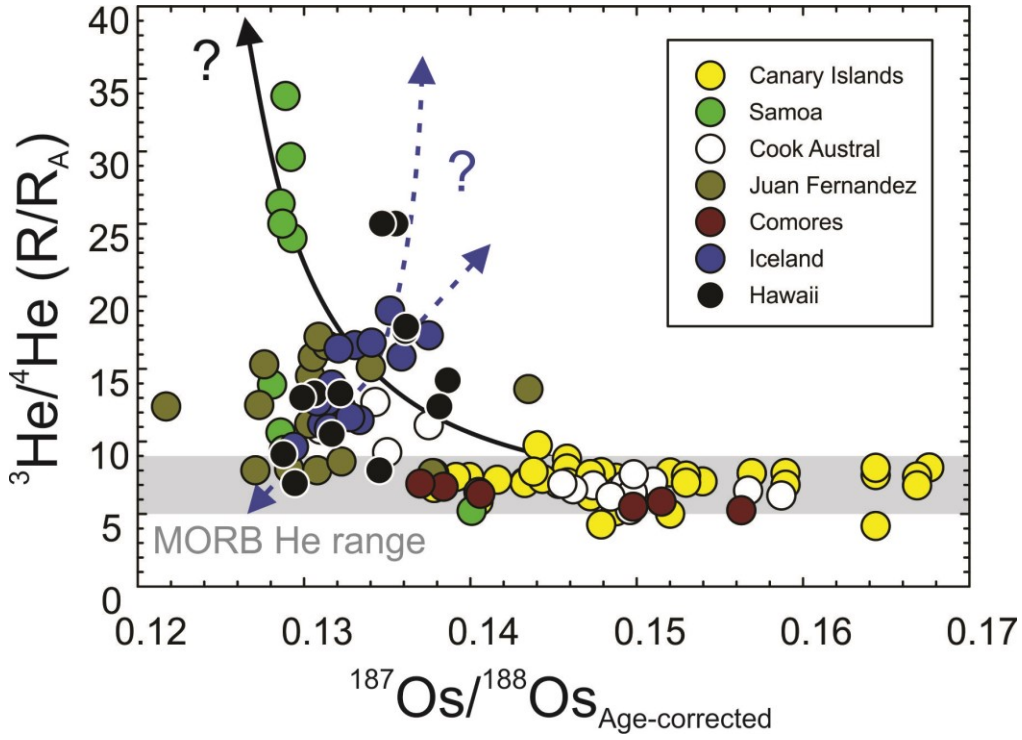

Figure 7: *Plot of $^{3}He/^{4}He$ from olivine separates versus $^{187}Os/^{188}Os$ in bulk rocks with >50 ppt Os for OIB. Denoted is the MORB range in He as well as possible mixing vectors between deep mantle radiogenic sources, like the core (blue lines) or mixing between radiogenic Os isotope reservoirs with MORB-like He, and high-$^{3}He/^{4}He$ mantle sources with primitive mantle-like Os isotopes (black line). Data are from Brandon et al. (1999; 2007), Class et al. (2009), Parai et al. (2009), Day & Hilton (2011), Day et al. (2010), Jackson & Shirey (2012) and Paquet et al. (2019), and references therein.*

To summarize section 4, OIB span a range of helium isotope compositions. Those with low- to MORB-like $^{3}He/^{4}He$ often have extreme radiogenic isotope flavors (EM, HIMU), with variable and sometimes radiogenic $^{187}Os/^{188}Os$ and $\mu^{182}W$ ~0, while OIB with intermediate- to high-$^{3}He/^{4}He$ converge to a more limited range of compositions, reflective of potentially early

differentiated and isolated sources with negative $\mu^{182}W$, and a limited range in Sr-Nd-Pb-Os isotope compositions, possibly reflecting core contributions (e.g., Brandon et al., 1999; Mundl-Petermeier et al., 2019), or simply ancient isolated mantle sources (e.g., Mundl et al., 2017). In certain cases, the relationships with He and other noble gases are not systematic within and between OIB, suggesting that other processes can complicate simple mixing relationships between sampled mantle reservoirs.

5. Unravelling solar and nucleogenic components in the deep mantle

Attempts to measure the neon isotope composition of oceanic basalts began in the mid-1970s (Craig & Lupton, 1975), but high-precision data only became available in 1988 with the publication of MORB data by Sarda et al. (1988). As mentioned previously, Ne is in low abundance in igneous rocks and their component minerals, but analytical challenges, especially related to $^{40}Ar^{++}$ and CO^{2++} interferences, make precise Ne isotope abundance measurements particularly difficult (see Moreira, 2013). Despite this, gas-rich samples have made broad characterization of MORB possible, as well as some OIB. Neon has three stable isotopes, ^{20}Ne and ^{22}Ne, and ^{21}Ne, which can be produced by reactions $^{24}Mg[n,\alpha]^{21}Ne$ and $^{18}O[n,\alpha]^{21}Ne$, respectively (Wetherill, 1954). Variations in $^{20}Ne/^{22}Ne$ have been interpreted to reflect contributions of a high $^{20}Ne/^{22}Ne$ solar component and of atmosphere ($^{20}Ne/^{22}Ne$ = 9.8; Sarda et al., 1988), whereas $^{21}Ne/^{22}Ne$ ratios are reflective of mixing between air ($^{21}Ne/^{22}Ne$ = 0.029), solar components, and nucleogenic products. Neon isotope space can therefore be described between the solar component, atmosphere (or air) and nucleogenic components which are all readily sampled in MORB (**Figure 8**). In this regard, it is notable that the $^{20}Ne/^{22}Ne$ of the MORB source appears to be lower than the OIB source value but what the exact $^{20}Ne/^{22}Ne$ value of the MORB source is and how it originates is still an open question - solar irradiated material, or solar nebula neon mixed in with chondritic neon during accretion, or solar nebula neon mixed in with atmospheric neon recycled through plate tectonics are all possibilities, discussed below.

Typically, three components are recognized; a solar wind component, with the highest $^{20}Ne/^{22}Ne$ (13.78; Heber et al., 2009), a solar nebula component derived by extrapolation (13.36; Heber et al., 2012) and a solar irradiation component with the lowest $^{20}Ne/^{22}Ne$, previously referred to as Ne-B (12.5; Black & Pepin, 1969) (**Figure 8**). The solar component is much debated due to the importance of this component for constraining accretion scenarios for the Earth (Marty, 2020).

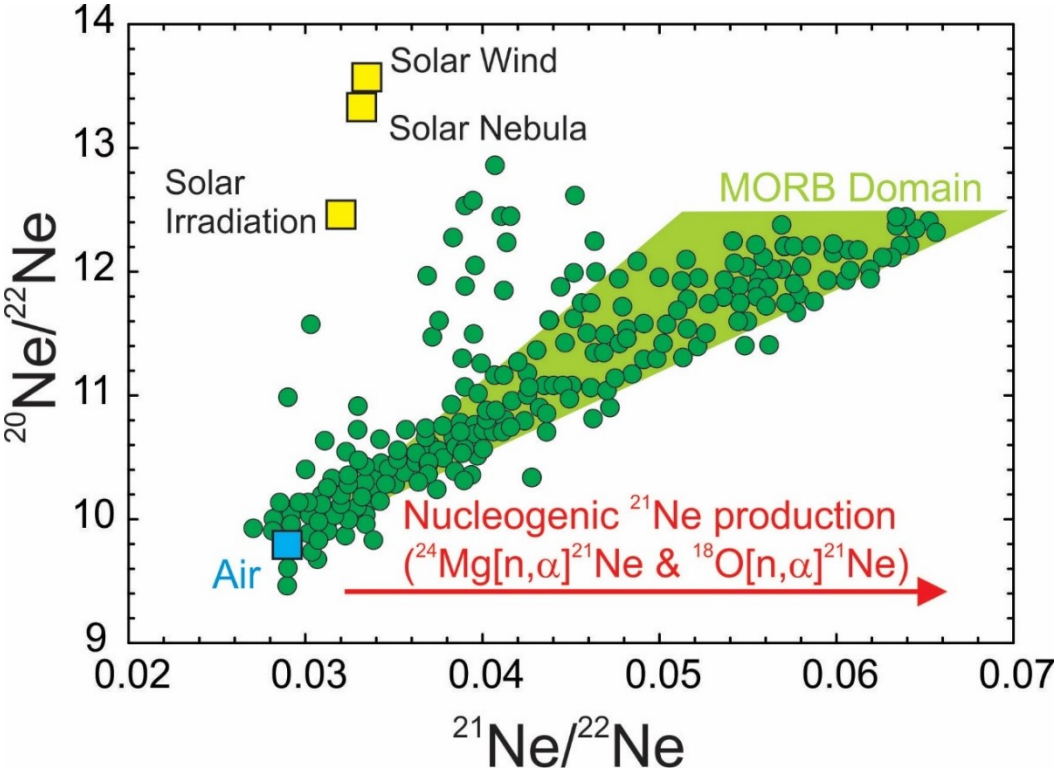

Figure 8: *Three-neon isotope plot for mid-ocean ridge basalts (green circles) versus the air (atmosphere) composition, and compositions of solar components. The Solar Nebula (SN) component is a likely candidate for early Earth composition, but the Solar Wind (SW) composition is often used for extrapolation to air-free compositions of ^{21}Ne/^{22}Ne. Samples of MORB show a range of nucleogenic ^{21}Ne/^{22}Ne components, with the average MORB domain taken from Moreira (2013). Data are from Moreira (2013) and references therein.*

Distinguishing between the possible endmembers is potentially important for understanding the relative contributions by noble gas addition to the Earth from a primary atmosphere with solar nebula composition (Harper & Jacobsen, 1996; Yokochi & Marty, 2004) and contributions of accreted materials with irradiated surfaces (Moreira & Charnoz, 2016; Peron et al., 2018). Discovery of OIB samples with ^{20}Ne/^{22}Ne ratios higher than the Ne-B component suggests that the former model must be at least partly correct (Williams & Mukhopadhyay, 2019). Choosing between these components is important, since extrapolations to atmosphere-free compositions are also derived for other isotopes (e.g., ^{21}Ne/^{22}Ne, ^{40}Ar/^{36}Ar) using this approximation. Since the largest value for the Solar Wind component generates the greatest variability in extrapolated compositions, we use this value for extrapolations presented in later figures.

Samples of MORB have been shown to be isotopically heterogenous with respect to Ne, but fall in a general MORB domain between air and a strongly nucleogenic component with $^{20}Ne/^{22}Ne$ up to ~12.5 (Sarda et al., 1988). Samples lying above the MORB domain shown in **Figure 8** are from the East Pacific Rise or Shona and Discovery rises in the South Atlantic and have high-$^{3}He/^{4}He$, with some of them being associated with tomographic anomalies, suggestive of 'non-normal' MORB (Moriera et al., 1995; Niedermann et al., 1997; Kurz et al., 2005). By comparison with MORB, most OIB samples show a restricted range in Ne isotope compositions, clustering close to the air value (**Figure 9**). As mentioned previously, this is due to the greater susceptibility to atmospheric contamination in lower Ne content OIB sample media (mainly olivine and pyroxene) compared with MORB glass. However, some studies have utilized glass samples and gas-rich cumulates to precisely define the Ne isotope characteristics of some OIB (e.g., Trieloff et al., 2000; Kurz et al., 2009; Jackson et al., 2009; Raqiun & Moreira, 2009; Mukhopadhyay, 2012; Peron et al., 2016; Williams & Mukhopadhyay, 2019). These studies have revealed that high-$^{3}He/^{4}He$ OIB, including Iceland, Fernandina in the Galapagos, Loihi Seamount in Hawaii, and Ofu in Samoa all have solar $^{20}Ne/^{22}Ne$ components, as do some intermediate-$^{3}He/^{4}He$ OIB such as Reunion, Kerguelen, and Pitcairn. Critically, the high-$^{3}He/^{4}He$ OIB have the steepest slopes in $^{20}Ne/^{22}Ne$-$^{21}Ne/^{22}Ne$ space, suggesting more limited nucleogenic components produced since the formation of their mantle reservoirs. A straightforward explanation for these differences between high-$^{3}He/^{4}He$ OIB and MORB is that nucleogenic Ne is produced in both reservoirs more or less equally, but that the concentration of noble gases in the high-$^{3}He/^{4}He$ OIB reservoir is higher. Alternatives including lower absolute abundances of radiogenic U and Th in high-$^{3}He/^{4}He$ mantle reservoirs do not seem tenable with Pb isotope systematics for these rocks. Partial melting may also play a role, where the high-$^{3}He/^{4}He$ OIB are generally tholeiitic, whereas OIB with lower-$^{3}He/^{4}He$ range from tholeiitic to strongly alkalic basalts.

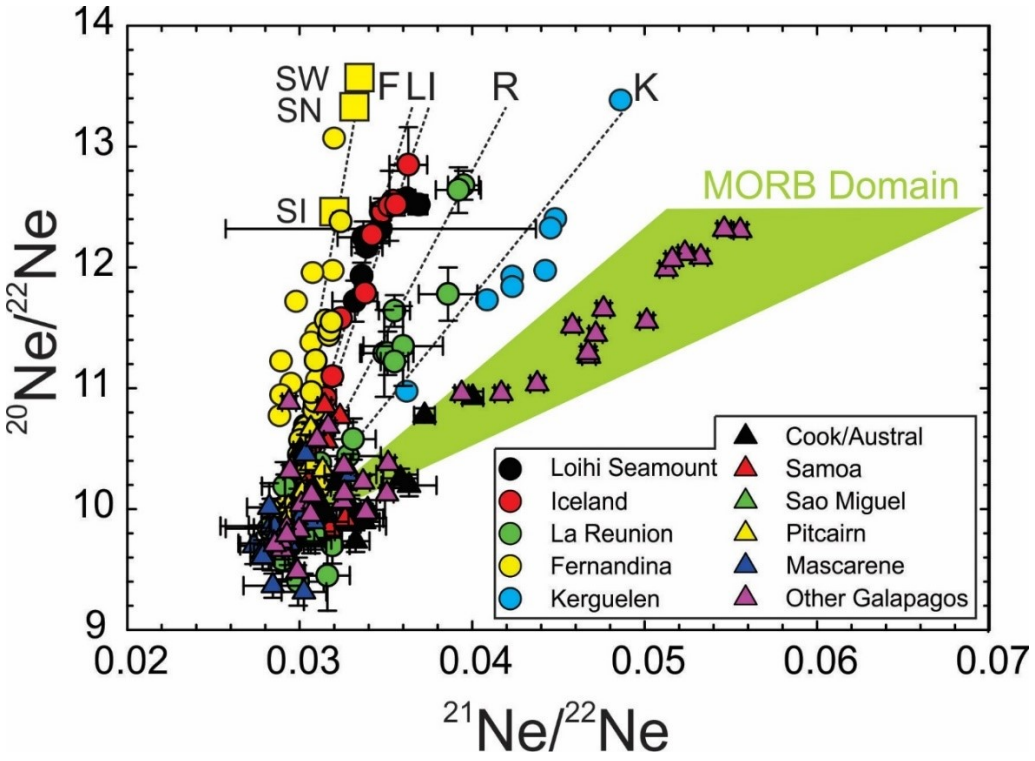

Figure 9: *Three-neon isotope plot for OIB with the same reservoirs shown in figure 8, but with abbreviations. Dashed lines are best fits through Fernandina (F), Loihi (L), Iceland (I), Reunion (R) and Kerguelen (K) data. SW, SN and SI stand for solar wind, solar nebula and solar irradiation components discussed in the text. Data are from Treiloff et al. (2000), Honda & Woodhead (2005), Parai et al. (2009), Jackson et al. (2009), Kurz et al. (2009), Hanyu et al. (2011), Lupton et al. (2012); Mukhopadhyay (2012), Moreira et al. (2012), Peto et al. (2013), Peron et al. (2017).*

Neon isotopes are inherently mixtures between a primary solar or source component and air, so that calculations can be made using an assumed $^{20}Ne/^{22}Ne$ composition to extrapolate to a $^{21}Ne/^{22}Ne$ ratio (in this case, 13.8). Doing this for OIB with resolvable $^{20}Ne/^{22}Ne$ values above the air value yields a range of $^{21}Ne/^{22}Ne_{ext}$ spanning from the nucleogenic MORB endmember, to near solar nebula compositions (**Figure 10**). Similar diagrams to **Figure 10** have been interpreted to reflect solar high-$^{3}He/^{4}He$ components in OIB (e.g., Jackson et al., 2009). In all the represented cases, $^{21}Ne/^{22}Ne_{ext}$ is lower than MORB, but the He isotope compositions can be variable and more radiogenic than in MORB, with Nd and Os isotope compositions often reaching compositions outside of the defined FOZO values for high-$^{3}He/^{4}He$ OIB. Nonetheless, the He-Ne correlation suggest a common, low $(U+Th)/^{3}He$, $(U+Th)/^{22}Ne$ source for OIB (Moriera, 2013), showing an early solar component in OIB sources, likely developed through nebula ingassing into the early Earth (e.g., Yokochi & Marty, 2004; Harper & Jacobsen, 1996; Mukhopadhyay 2012; Williams & Mukhopadhyay, 2019).

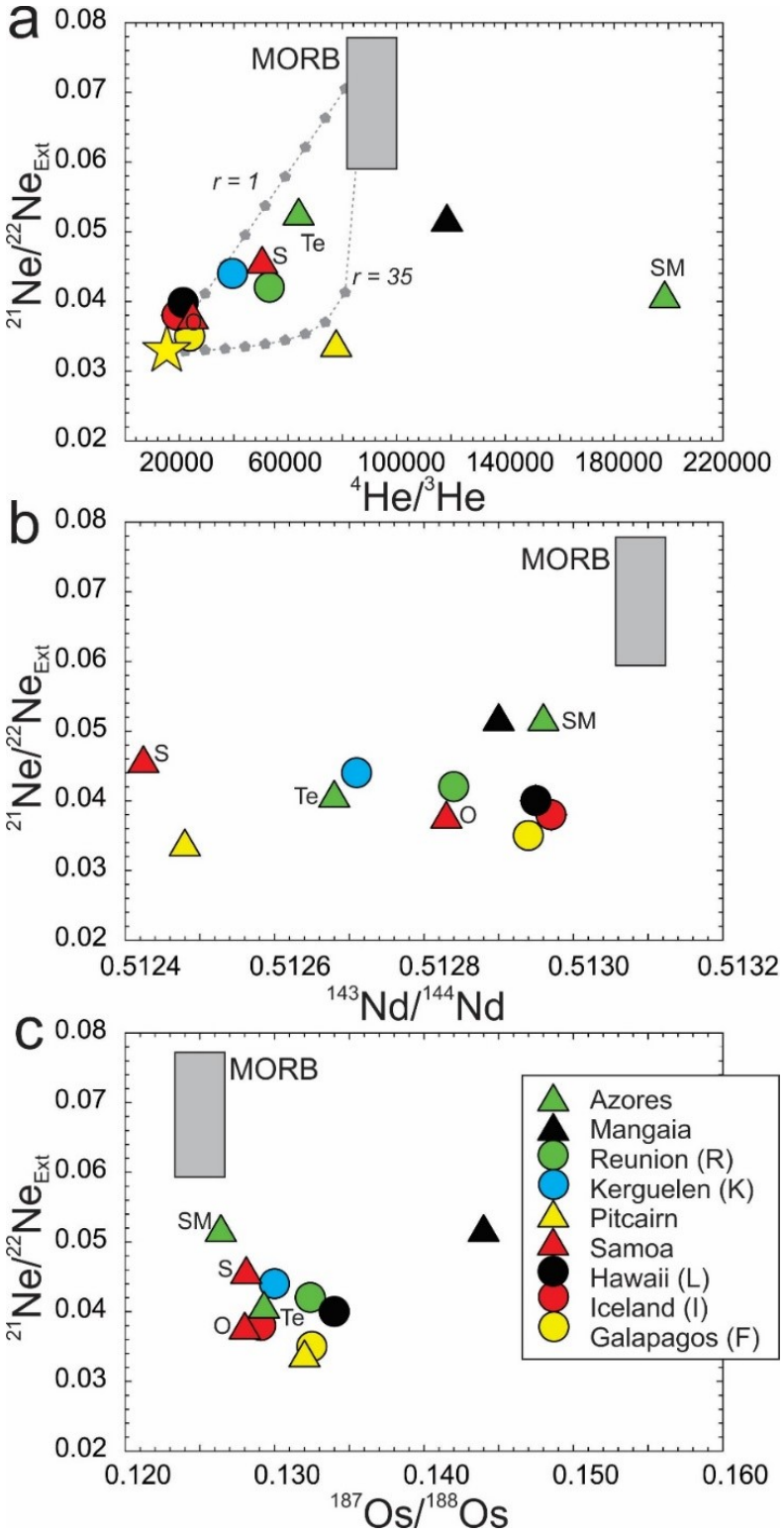

Figure 10: *Extrapolated $^{21}Ne/^{22}Ne$ versus He, Nd and Os isotope compositions in OIB. Data sources are given in Table 1. Abbreviations are for individual islands: SM = Sao Miguel, Azores; Te = Teceira, Azores; O = Ofu, Samoa; S = Savaii, Hawaii.*

This component has subsequently been degassed extensively from the mantle sampled during upwelling beneath ridges and, prior to this, during the formation of the continents, whereas isolated deep mantle sources have been less affected by these processes. Even so, Ne isotopes hint at less-clear associations with Sr-Nd-Pb-Os isotopes. For example, low $^{143}Nd/^{144}Nd$ is associated with low Sm/Nd crustal reservoirs. These relationships suggest that He and Ne isotope signatures in OIB can be mixed with subducted components, and so noble gases might be decoupled in some - perhaps even most – instances from their radiogenic isotope compositions. Heavier noble gases allow consideration of this issue.

6. Mantle outgassing and heavy noble gases

Of the remaining noble gases, isotopic data for Ar are the most common in OIB samples, with Kr isotope data being essentially absent. Remarkable analytical efforts, and the selection of key samples, have also enabled high-precision analyses of Xe isotopes. Argon has three stable isotopes, ^{36}Ar, ^{38}Ar, and ^{40}Ar. Argon-40 is produced by decay of ^{40}K and is now the most abundant isotope of Ar in the Earth. The atmosphere is composed of 0.93% Ar, with a $^{40}Ar/^{36}Ar$ ratio of 295.6, so all samples measured for Ar represent mixtures between the atmospheric composition and a solar component modified by ingrowth of ^{40}Ar. As with Ne, extrapolation of $^{40}Ar/^{36}Ar$ and $^{38}Ar/^{36}Ar$ ratios to the solar component are done versus the $^{20}Ne/^{22}Ne$ measured for the same samples (see, for example, Mukhopadhyay & Parai, 2019). These extrapolations for $^{38}Ar/^{36}Ar$ suggest a solar component to OIB (e.g., Raquin & Moreira, 2009; Peron et al., 2017) and the lower time-integrated $^{40}K/^{36}Ar$ ratio calculated for OIB are consistent with sampling of mantle sources that have experienced less processing and degassing over Earth history than the depleted MORB mantle.

A similar procedure can be done for Xe, which has nine stable isotopes, of which ^{129}Xe was produced by decay of the extinct radionuclide ^{129}I ($T^{1/2}$ = 16 Myr) in the first ~100 million years of Solar System history, and several other isotopes (^{131}Xe, ^{132}Xe, ^{134}Xe, ^{136}Xe) were formed by either spontaneous fission of ^{244}Pu ($T^{1/2}$ = 82 Myr) in the first ~500 million years of the Solar System or are presently being produced by spontaneous fission of ^{238}U ($T^{1/2}$ = 4.47 Gyr) (Marty, 2020). While somewhat complicated, Xe isotopes have the power to unravel a range of processes, pointing to Xe loss from the atmosphere by preferential ionization (Zahnle et al., 2019; the 1st Xe paradox of Marty, 2020), the existence of several distinct sources of Xe within the Earth (Marty,

1989), or possible delivery of ^{129}Xe-rich material to the Earth after mantle degassing (2nd Xe paradox of Marty, 2020), and the potential for variable differentiation or late stage heterogeneous volatile accretion to the Earth from Pu/I ratios obtained from Xe (Parai & Mukhopadhyay, 2015; 3rd Xe paradox of Marty, 2020). For simplification, only ^{129}Xe/^{130}Xe data for OIB are considered here and for a fuller consideration of Xe isotopes in OIB, the reader is referred to Mukhopadhyay & Parai (2019) and Parai et al. (2019).

As with Ne and Ar, ^{129}Xe/^{130}Xe$_{ext}$ is corrected for atmospheric contamination using a variety of extrapolation methods (see Mukhopadhyay, 2012). Here, we take data extrapolated in studies of MORB and four OIB locations (**Figure 11**). The MORB data are for glass samples with relatively high Xe, while the OIB data are from distinct glasses (e.g., the Iceland DICE sample; Mukhopadhyay, 2012), or cumulate rocks with high Xe contents (Treiloff et al., 2000). An important feature of the OIB data is that the ^{21}Ne/^{22}Ne$_{ext}$, ^{40}Ar/^{36}Ar$_{ext}$ and ^{129}Xe/^{130}Xe$_{ext}$ are all lower than the MORB values. These would suggest that the high-^{3}He/^{4}He mantle reservoir has distinct Ne, Ar and Xe isotope characteristics and is distinct from the mantle sampled by MORB.

A complication in the study of heavier noble gases is subduction. Because heavier noble gases, especially Xe, are more soluble in water than He, subduction of these gases into the mantle is all but assured. How efficiently these gases are returned to Earth's interior by subduction is not well-constrained, but evidence for this process has been made evident by discovery of non-radiogenic Xe signatures in the atmosphere and in CO_2 well gases (Cafee et al., 1999; Holland & Ballentine, 2006). For OIB, Treiloff et al. (2002) showed that non-radiogenic isotopes of Xe in Iceland, Reunion and Loihi Seamount were close to atmospheric ratios, rather than having solar compositions, consistent with significant subducted Xe in their sources. Mukhopadhyay (2012) was able to show that the lower ^{129}Xe/^{130}Xe ratios result from a lower I/Xe ratio in the source of Icelandic basalts and cannot be explained solely by mixing atmospheric Xe with MORB-type Xe. This, in turn, suggests early isolation of the OIB source reservoir, which was then mixed in limited quantities with the upper mantle. Despite these observations, substantial subduction of seawater-derived noble gases into the convective mantle has occurred such that 80 to 90% of the Xe in both OIB and MORB is recycled from the atmosphere (Parai & Mukhopadhyay 2015, Tucker et al. 2012). Clear separation of this subduction signature in OIB from signatures from mixing with the MORB source strongly implicates atmospheric Xe reaching the deep Earth with deeply subducted slabs.

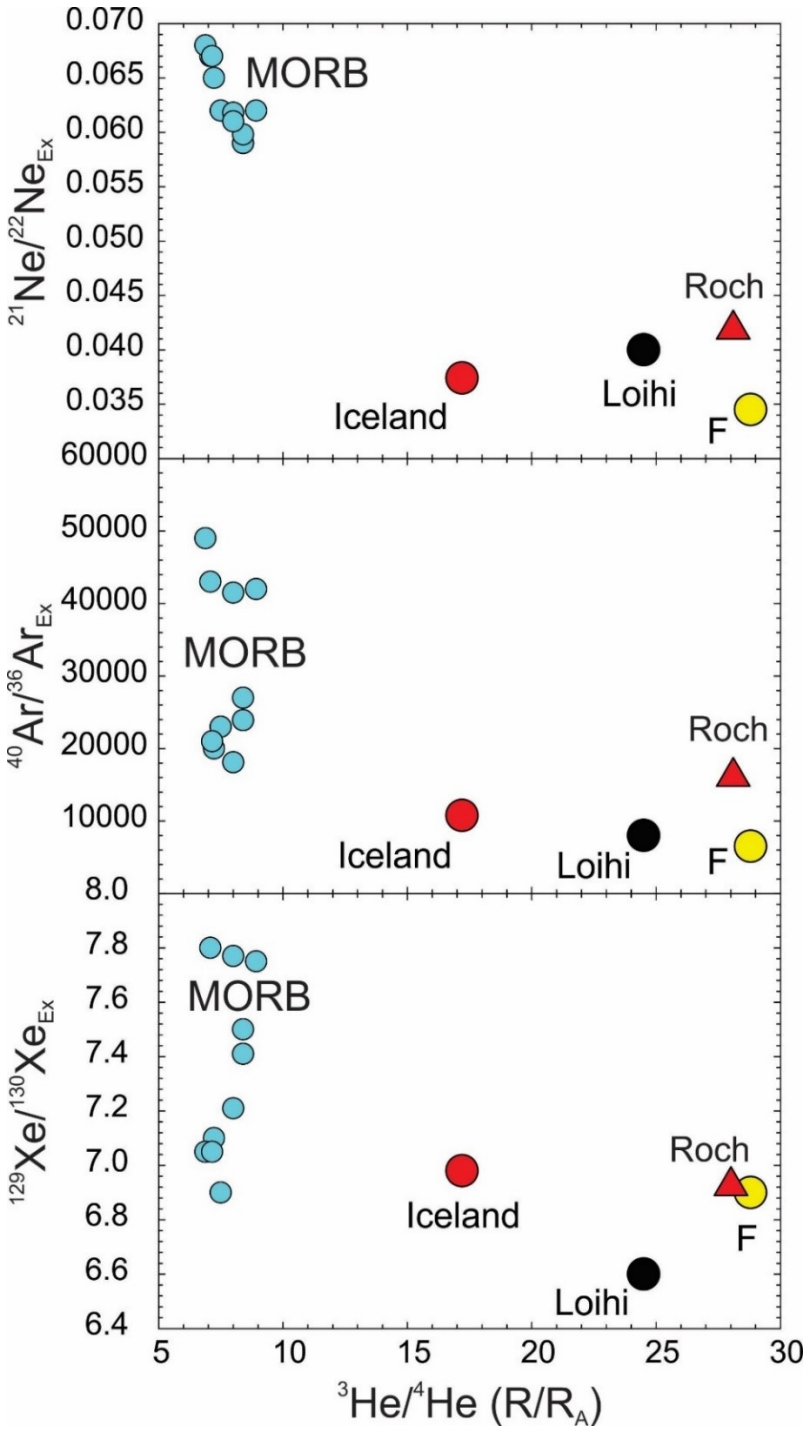

654

655 ***Figure 11:*** *Helium isotope composition versus extrapolated Ne, Ar and Xe isotope compositions*
656 *for the four high-$^{3}He/^{4}He$ OIB localities (Iceland, Loihi [Hawaii], Fernandina [Galapagos] and*
657 *Rochambeau [Samoa]) versus MORB samples. Loihi and Fernandina data points are not as well*
658 *determined as Iceland or Rochambeau (Samoa) because the mixing hyperbolas are weakly*
659 *constrained. Data are from Moreira et al. (1998), Treiloff et al. (2000), Parai et al. (2012), Tucker*
660 *et al. (2012), Mukhopadhyay (2012), Peto et al. (2013), Peron et al. (2017) and Parai &*
661 *Mukhopadhyay (2021).*

7. Evidence for recycled components in FOZO

The heavier noble gases and most critically, Xe, provide overwhelming evidence for subducted noble gas components in mantle reservoirs (Cafee et al., 1999; Holland & Ballentine, 2006), and more specifically, in OIB (Treiloff et al., 2002; Mukhopadhyay, 2012; Mukhopadhyay & Parai, 2019; Parai et al., 2019). These lines of evidence can be used to construct a mass balance of Xe replenishment into the mantle (Moreira, 2013) and are powerful tools for understanding early atmospheric degassing. For example, subduction of atmospheric Xe into the mantle source of MORB implies very high $^{129}Xe/^{130}Xe$ (>25) in the mantle ~4.4 billion years ago (Staudacher & Allegre, 1988; Parai et al., 2021). This is most easily explained by massive Xe loss, possibly associated with an ocean's worth of water loss - if Xe loss was a continuous process - in the Early Earth (Zahnle et al., 2019), resulting in a very high $^{129}I/^{130}Xe$ ratio in the mantle. Consequently, pollution of the mantle by subducted gases from the atmosphere with low $^{129}Xe/^{130}Xe$ has taken place, reducing the $^{129}Xe/^{130}Xe$ in both the MORB and OIB mantle sources (e.g., Moriera, 2013). In addition to recycled atmospheric Xe, some OIB sources exhibit high ratios of Pu-fission Xe to U-fission Xe independently supporting less degassing of OIB sources relative to MORB sources (Parai et al., 2019).

Evidence for recycled components from radiogenic isotopes in OIB sources has long been known (e.g., Gast et al., 1964; White & Hofmann, 1982). This is particularly well accepted in low- and MORB-like-$^{3}He/^{4}He$ OIB (8 ±2 R_A) which can have extreme HIMU or EM signatures (e.g., Chauvel et al., 1992; Woodhead et al., 1996; Elliott et al., 2007; Day et al., 2010). However, significant debate surrounds whether recycled components exist in the FOZO reservoir. Some have argued, based on radiogenic isotopes, that FOZO is a primary early isolated and geochemical depleted reservoir in the mantle (Hart et al., 1993). In a recent iteration, this reservoir has been suggested to be the mantle region least affected by recycled crust (Jackson et al., 2020). On the other hand, all known OIB, including those with high-$^{3}He/^{4}He$, define a slope in $^{207}Pb/^{204}Pb$–$^{206}Pb/^{204}Pb$ space that lies to the right of the geochron, representing mixing of the mantle from Archaean to present-day (Hofmann, 2003). These observations support the notion that OIB are not formed by simple mixing between depleted and enriched mantle components but may instead sample a mantle that is 'marble-caked' (c.f., Allegre & Turcotte, 1986), and has experienced multiple enrichment events from recycled ocean crust and lithosphere. Differences in isotopic compositions between OIB and MORB could also partly reflect lower degrees of partial melting

693 for OIB, and preferential melting of enriched mantle components, versus large-degrees of
694 decompression melting of DMM and dilution of enriched signatures in the case of MORB (Day et
695 al., 2010). In this scenario, the three major enriched mantle components in OIB (HIMU, EM1,
696 EM2; Zindler and Hart, 1986) represent recycled materials which are relatively unmixed in the
697 mantle compared with older heterogeneities generated through subduction, which have been more
698 effectively mixed into the mantle (to form the 'C', 'FOZO', or 'PHEM' component(s)).

699 Heavy noble gas isotopes support the latter model. As pointed out by Parai et al. (2019)
700 and Mukhopadhyay & Parai (2019), OIB with high-$^{3}He/^{4}He$ and solar-like Ne isotopic
701 compositions should not be interpreted to reflect sampling of pristine, isolated mantle reservoirs
702 and so lithophile isotope compositions of such samples should not be taken to represent
703 undifferentiated mantle either. To illustrate this point, comparison is made between $^{129}Xe/^{130}Xe$
704 and $^{187}Os/^{188}Os$ (**Figure 12**). These data have not been measured on the same materials, so
705 extrapolation of Xe and estimation of the dominant $^{187}Os/^{188}Os$ signature is necessary. This is
706 performed using the estimates of Xe given in Mukhopadhyay & Parai (2019) and by taking age-
707 corrected $^{187}Os/^{188}Os$ in the most primitive basalts from the respective locations (given in Day,
708 2013; Gibson et al., 2016). For the depleted MORB mantle, estimates of Xe isotope composition
709 are taken from Parai et al. (2012), Tucker et al. (2012), and Parai & Mukhopadhyay (2021), and
710 for Os, estimates are taken from the range in abyssal peridotite compositions since MORB glasses
711 typically record radiogenic Os isotope compositions due to their low Os abundances and
712 susceptibility to seawater contamination. The four high-$^{3}He/^{4}He$ OIB have consistently more
713 radiogenic $^{187}Os/^{188}Os$ than DMM. The long-term Re/Os ratio of the bulk silicate Earth (0.1296;
714 Meisel et al., 1996) is higher than that of DMM (~0.126; Day et al., 2017), due to melting of the
715 MORB source and loss of Re over time. However, four OIB locations have different $^{187}Os/^{188}Os$
716 ratios, with Fernandina (Galapagos) and Loihi (Hawaii) in particular, having compositions above
717 this value. The heterogeneity in Os isotopes in these high-$^{3}He/^{4}He$ OIB can be readily explained
718 by addition of radiogenic Os from subducted components and mixing with isolated mantle
719 reservoirs. The consistently radiogenic $^{187}Os/^{188}Os$ in Icelandic, Loihi, Samoa and Galapagos lavas
720 are not well explained by their mantle reservoirs representing depleted components relatively
721 unaffected by recycled crust.

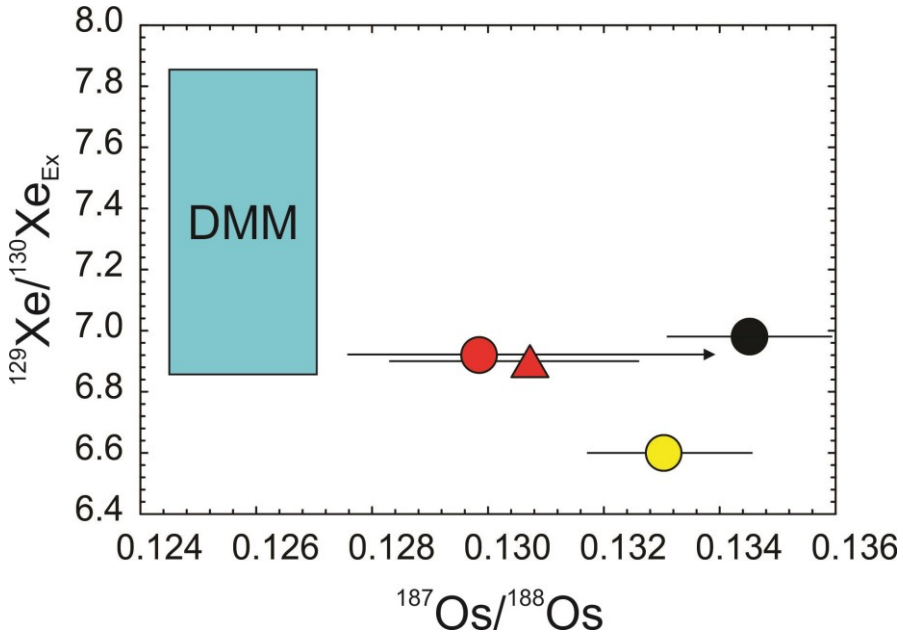

Figure 12: *Osmium versus xenon isotope data for Iceland (red circle), Loihi (black circle), Samoa (red triangle) and Fernandina (yellow circle). The $^{129}Xe/^{130}Xe$ data are extrapolated values given in Treiloff et al. (2000), Mukhopadhyay (2012), Peto et al. (2013), and Peron et al. (2017), and $^{187}Os/^{188}Os$ data are the average of the most primitive (high-MgO) samples from each island, given in Brandon et al. (1999; 2007), Jackson & Shirey (2012) and Gibson et al. (2016). The DMM values are from Figure 11 for Xe and from the average DMM composition (Day et al. 2017). The greatest extrapolation between samples is for the Samoa source, using island data and the Rochambeau Xe. Arrow on the error bar for Samoa represents the presence of radiogenic $^{187}Os/^{188}Os$ components possible in the plume.*

Further support for recycled components in FOZO sources comes from oxygen fugacity (fO_2) estimates of OIB. To date, all OIB measured for their fO_2 have been found to be more oxidized than MORB, using either XANES (Brounce et al. 2017; Helz et al. 2017; Moussallam et al., 2014; 2016; 2019) or V-in-olivine oxybarometry (Nicklas et al., 2019). Lack of correlations with Sr-Nd-Pb isotope signatures has been interpreted to represent volumetrically minor trace element enriched mantle lithologies dominating radiogenic isotopes, while fO_2 reflects the volumetrically dominant mantle component. In turn, high fO_2 in OIB relative to MORB implies a uniformly oxidizing plume source mantle that may be the result of either a common oxidized oceanic crust-rich reservoir parental to modern plume lavas, or preservation of un-degassed and oxidized mantle domains formed early in Earth history. Comparison of V-in-olivine oxybarometry for the same olivine populations measured for $^{3}He/^{4}He$ for a range of OIB, including from low- to high-$^{3}He/^{4}He$ examples show that all are oxidized (**Figure 13**). This demonstrates that even the FOZO reservoir is oxidized relative to MORB. Given the evidence for recycled signatures in Xe

and Os, therefore, the oxidized nature of FOZO OIB possibly relates to recycling. Evidence from ancient Xe signatures, combined with a Xe budget dominated by recycled components indicates that high-$^3He/^4He$ OIB cannot sample only unprocessed ancient (>4.45 Ga) regions of the mantle (e.g., Mukhopadhyay & Parai, 2019). Evidence from Xe, radiogenic Os isotope data and fO_2 constraints, suggests that recycled material is mixed in with ancient mantle sources, such that OIB sources are not convectively isolated.

In this sense, FOZO is likely to be a heterogeneous mixture of different components and that partial melting is likely to bias isotope compositions of lavas away from that of their source. As such, FOZO may not be a physically distinct reservoir, but rather a combination of variable mixing and preferential sampling during partial melting. The prior divide of high- and low-$^3He/^4He$ mantle sources may be merely an artifact of assessing OIB from their maximum He values, rather than examining their true He-isotope variation.

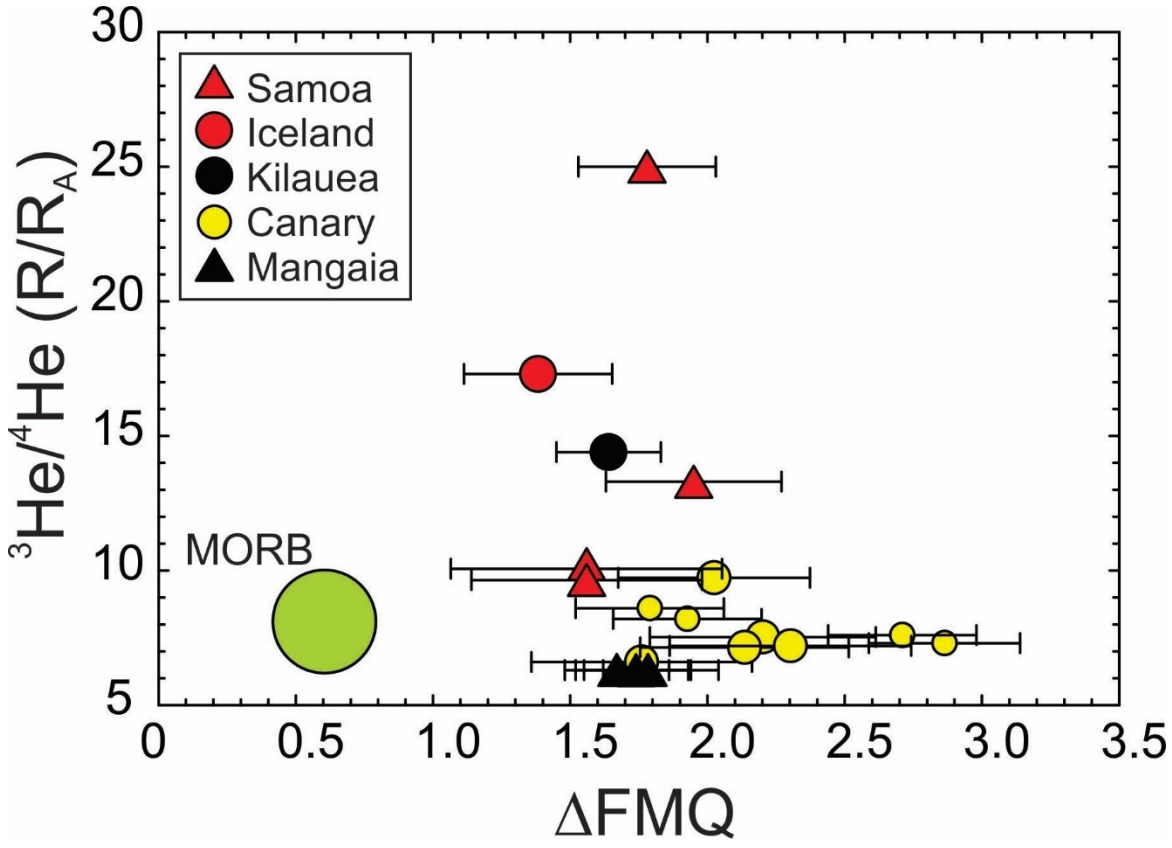

Figure 13: *Oxygen fugacity estimates, relative to the fayalite-magnetite-quartz redox buffer, using the V-in-Olivine oxybarometer, versus $^3He/^4He$ in olivine for OIB versus MORB. Data for He isotopes are given in Brandon et al. (2007), Day & Hilton (2011), Jackson et al. (2007) and for MORB are from Graham (2002). Data for V-in-Olivine are from Nicklas et al. (2019; in review).*

8. Linking noble gases, mantle structure and mantle geodynamics

In recent years, renewed efforts have been made to link He isotopes to mantle structure (Jackson et al., 2017; Jones et al., 2019; Williams et al., 2019). Such studies have recognized links with hotter plumes from seismically slow regions of the mantle and high-$^{3}He/^{4}He$. Hotter plumes also imply differences in degrees of partial melting at Earth's surface, and this has long been known from differences in basalt petrology between dominantly tholeiitic magmatism in Iceland and Hawaii main shield volcanoes, versus dominantly alkali basaltic magmatism in many other OIB. This relationship is captured to a lesser or greater extent in buoyancy fluxes beneath OIB, most recently computed by Hoggard et al. (2020). A notable feature of buoyancy fluxes and maximum $^{3}He/^{4}He$ ratios in OIB are that they broadly positively correlate (**Figure 14**). Relationships between buoyancy flux and extrapolated $^{21}Ne/^{22}Ne$ are not as systematic, with several low-$^{3}He/^{4}He$ plumes having low $^{21}Ne/^{22}Ne_{ex}$; possibly even lower than high-$^{3}He/^{4}He$ OIB (**Figure 14**). These relationships would support the hypothesis of the hottest plumes sourcing the highest $^{3}He/^{4}He$ OIB (Jackson et al., 2017), which contain some early isolated components with solar Ne compositions, but would also equally support some early isolated components being present in low-$^{3}He/^{4}He$ OIB with lower buoyancy fluxes.

In this sense, these relationships are consistent with earlier models by Gonnermann & Mukhopadhyay (2009) who showed that mantle He-Nd isotope systematics could be explained by differential incorporation of He-poor recycled slabs (e.g., Moriera & Kurz, 2001; Day et al., 2015) with high Sm/Nd ratios into both the MORB and OIB sources over Earth history. The ^{3}He-depleted slabs with atmospheric Xe mix with ancient reservoirs, diluting concentrations of solar-like Ne and Ar and high $^{129}Xe/^{130}Xe$ and, due to reduced total gas contents, decreasing the efficiency of subsequent mantle degassing while imparting depleted lithophile compositions to the mantle reservoir (Gonnermann & Mukhopadhyay 2009). Consequently, mixing of slabs and ancient reservoirs would generate a continuum of compositions between relatively well-mixed assemblages and incompletely mixed recycled slabs as suggested by OIB with a range of maximum $^{3}He/^{4}He$. Differences between OIB and MORB sources could relate to the greater degree of processing and mixing in MORB source mantle, with limited direct mixing between the two to preserve differences in radiogenic Xe produced by extinct radionuclides (Mukhpadhyay & Parai, 2019). Combined with variable degrees of partial melting in the OIB source mantle, these

complex relationships can explain much if not all the noble gas and radiogenic isotope (Sr-Nd-Hf-W-Os-Pb) isotope systematics of OIB. While many models favor using the most extreme high-$^{3}He/^{4}He$ signatures of OIB, differential partial melting and heterogeneous mantle sources would also allow the incorporation of isotopic heterogeneities within island chains, explaining why He and Ne isotope compositions in locations like the Azores, Canary Islands, Hawaii, Iceland or Samoa can be so variable.

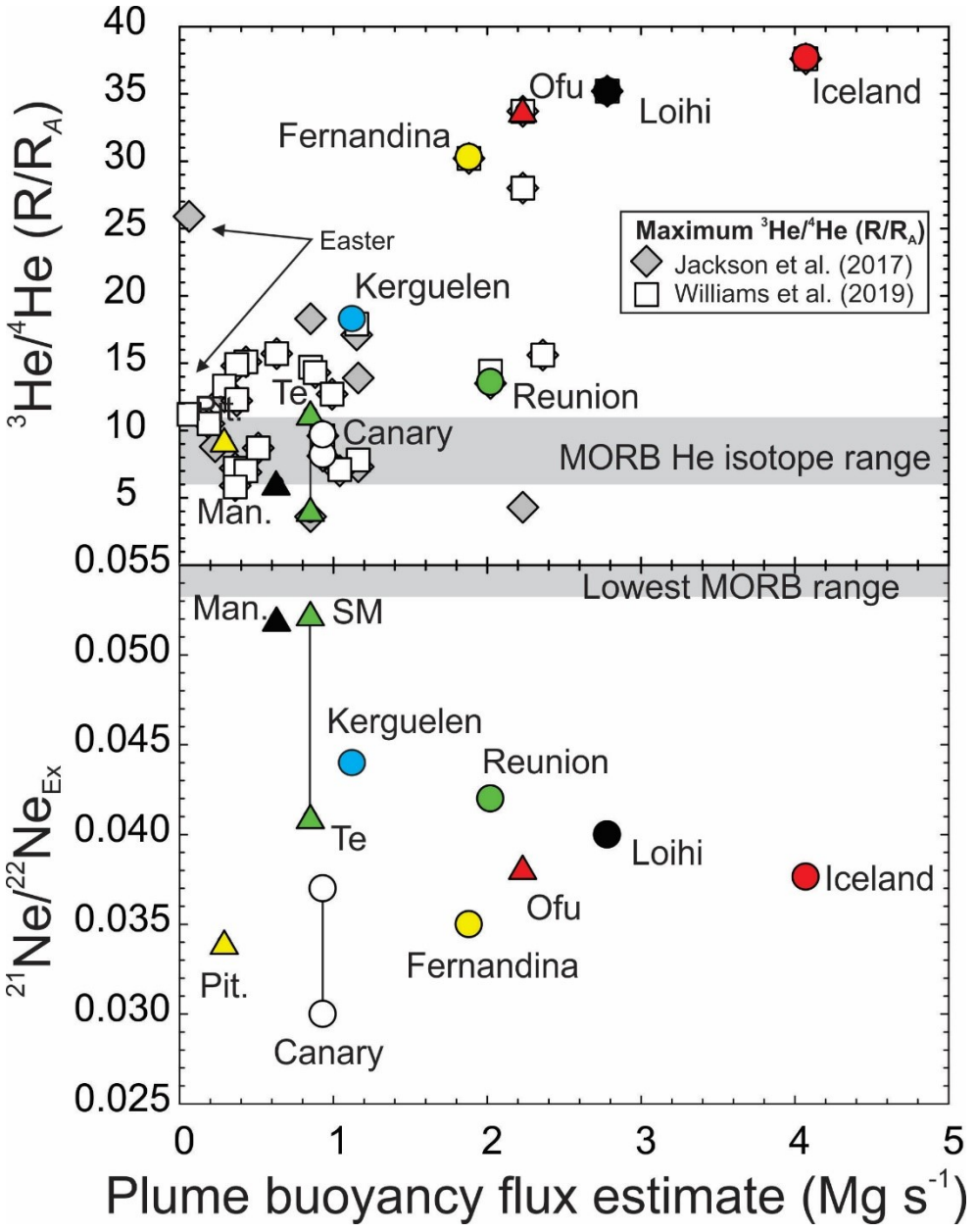

Figure 14: *Plume buoyancy flux, taken from the recent estimates of Hoggard et al. (2020) for ocean island chains, versus maximum $^{3}He/^{4}He$ ratios in OIB and extrapolated $^{21}Ne/^{22}Ne$, given in*

Table 2. Since the highest $^{3}He/^{4}He$ ratios are normally restricted to individual locations, these are shown, where possible, with abbreviations of Te and SM representing Terceira and Sao Miguel in the Azores. The MORB He and NeEx ranges are from Graham (2002) and estimates given in Figure 11. Note, different maximum $^{3}He/^{4}He$ ratios exist for different studies, for example Easter. In this later case it is due to the addition of unpublished data in the compilation of Jackson et al. (2017).

So far, the discussion in this paper has considered what *can* melt during the formation of OIB, rather than what *cannot* melt. Stracke and others have made compelling arguments that refractory components more depleted than DMM exist, that *cannot* melt at typical mantle potential temperatures for OIB (e.g., Stracke et al., 2019). Such refractory or depleted components are likely to form through prior partial melting events in Earth and are readily returned to the convecting mantle. The most likely mode for this in the modern Earth is through plate tectonics, as such depleted components may be low-$^{3}He/^{4}He$ oceanic lithosphere, which can have radiogenic Nd and Hf and unradiogenic Os (e.g., Day et al., 2017). Evidence for these components in OIB are rare and have been reported as melt inclusions with highly depleted compositions (Stracke et al., 2019), or as strongly depleted components in Icelandic basalts that are the products of unusually high-degrees of partial melting (Stracke et al., 2003).

Models recreating mantle heterogeneity as a function of melting processes at Earth's surface predict that refractory components in the mantle both increase over time and are significant components in the mantle (Jones & Day, 2021). These models incorporate ancient, deep mantle reservoirs and show the secular evolution of the mantle enables greater sampling of these features over time (**Figure 15**). Such models recreate a 'marble-caked' mantle (Turcotte & Allegre, 1986) and, relevant to OIB, they predict both plumes that come from the deep mantle, possibly at the apices of early isolated mantle reservoirs, as well as from surrounding mantle regions without the strong input from such reservoirs. In most senses, these models appear to recreate snapshots of the Earth preserved in seismic tomography images (e.g., Jones et al., 2020).

In addition to down-going recycled basaltic crust, models predict down-going depleted peridotite lithosphere as well as significant mixing between refractory and enriched (basaltic slab) components. This is, in essence, an identical picture to that currently painted by noble gas and radiogenic isotopes in OIB. An example interpretation of a convection model is given in **Figure 16**. Simulations strongly suggest that even the high-$^{3}He/^{4}He$ OIB contain significant recycled components, and that the depleted nature of the FOZO reservoir may equally be a consequence of

recycling and mixing processes within the deep Earth. The strongest lines of evidence supporting early isolated reservoirs in the mantle remain high-$^{3}He/^{4}He$, solar Ne, Ar and Xe and negative $\mu^{182}W$ anomalies in some OIB, but these signatures are likely to be heterogeneously mixed, depending on temperature and viscosity contrasts of upwelling plumes. Due to higher temperatures, larger viscosity contrasts in the early mantle relative to the modern mantle might also suggests that these isolated components were not as easily accessed in the early Earth. Future work is required to understand the true missing components in OIB – the refractory mantle signatures that are absent or overlooked – and how these signatures bias current views of OIB geochemistry, both for the noble gases as well as for radiogenic and stable isotope signatures.

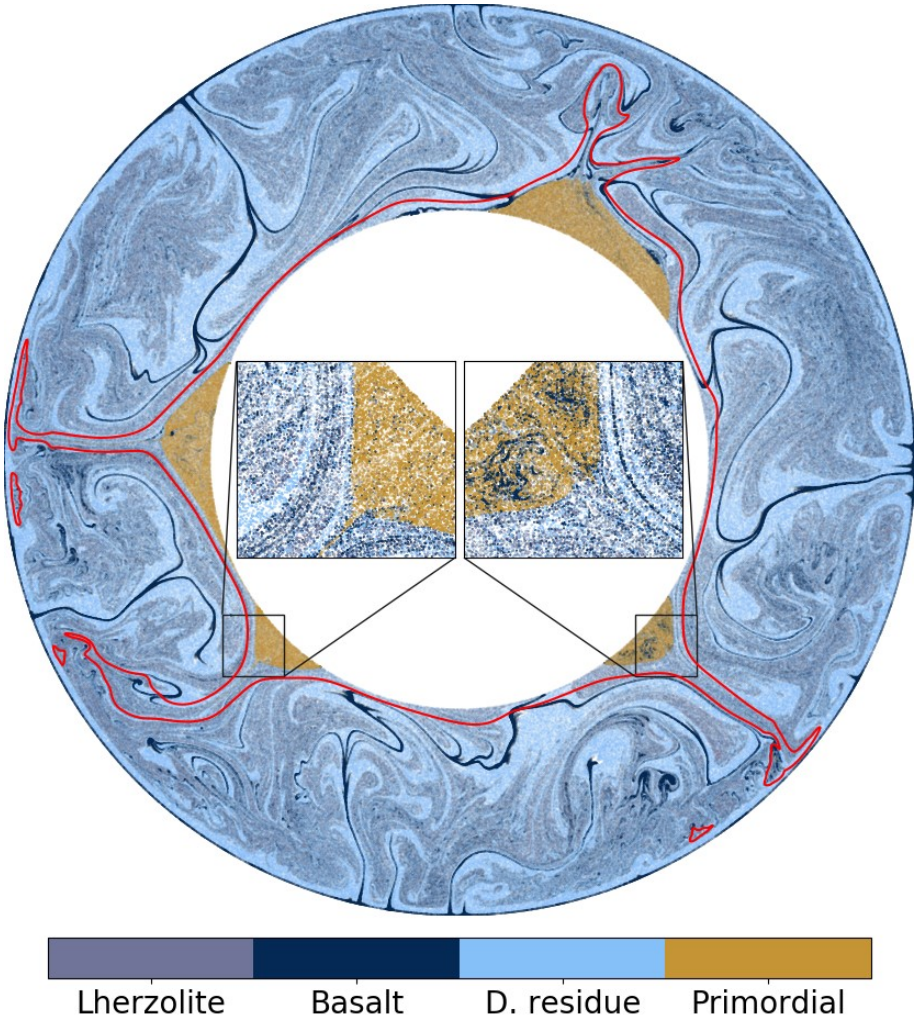

Figure 15: *2-D model of mixing processes between fertile mantle (lherzolite) and primordial reservoirs, refractory mantle components (D. residue or depleted residue) and subducted basalt (basalt) at a snap shot in time. Interpretation of this computational model specifically for the noble*

gases is given in Figure 16. Shown in the inset are mixing relations with the primordial, recycled basalts and depleted residue. These simulations predict mixing of these components into such reservoirs, consistent with noble gas evidence for recycled components with early-formed mantle heterogeneities. Temperature contour at 1673 K in red.

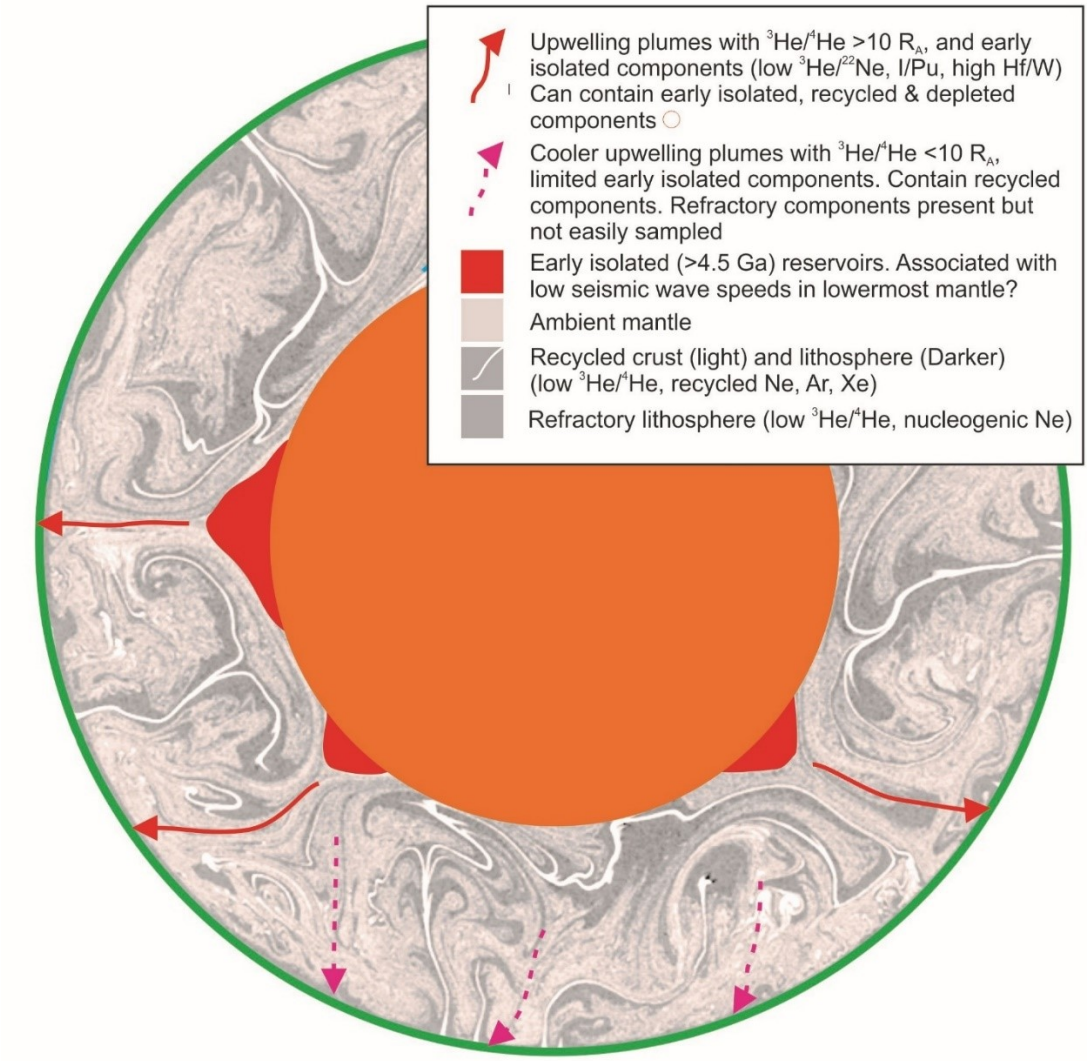

Figure 16: *Possible interpretation of figure 15 in the context of noble gas isotope systematics in OIB. Note the significant refractory components in OIB. This refractory lithosphere should have low-$^3He/^4He$ (e.g., Moriera & Kurz, 2001) as well as nucleogenic Ne, by virtue of low initial Ne gas contents and reactions on Mg and O in these ultramafic rocks.*

Conclusions and Outlook

This examination of available noble gas systematics in OIB draws the following conclusions:

1. Consideration of sample media (glass, minerals, hydrothermal gases and fluids) is important both for recognizing primary mantle components, but also for understanding spatial and temporal variations in noble gases within OIB. Taking these and other issues related to noble

gas sampling into account will be especially important as machine learning techniques are increasingly employed to investigate variations within large geochemical datasets, so as not to obtain erroneous results.

2. The degree of partial melting producing OIB is critical. Low-degree partial melting will lead to preferential sampling of more fusible and generally enriched components, while high-degree melts will dilute these components with more melts of more refractory components.
3. Diffusion of the noble gases is likely to be faster in the mantle than for other commonly measured isotopes (e.g., O, Sr, Nd, Hf, W, Os, Pb). Diffusion may be important for decoupling of noble gases from other isotope systems. Determining the role of diffusional processes on the distribution of noble gases within both OIB and MORB remains an important area of research.
4. OIB with low- and MORB-like $^{3}He/^{4}He$ are dominantly sampling mantle domains from the convecting mantle but can also contain some relatively undegassed (solar) components. Their range in Sr-Nd-Os-Pb isotope compositions reflect a strong recycled heritage.
5. OIB with intermediate to high-$^{3}He/^{4}He$, especially Loihi (Hawaii), Iceland, Fernandina (Galapagos) and Ofu (Samoa) preserve evidence for sampling a reservoir that has been relatively isolated since ~4.5 billion years from noble gases (He, Ne, Ar, Xe) as well as from W isotopes. However, this reservoir is not pristine and these OIB show strong evidence for containing both depleted and enriched recycled components.
6. Linking the highest-$^{3}He/^{4}He$ OIB to FOZO: the FOZO reservoir is not a reservoir least affected by recycling of crust, rather it is a mantle reservoir that contains recycled components including depleted lithosphere. This difference in definition means that, while the FOZO reservoir is almost certainly sampled by the deepest, hottest mantle plumes, its status as a primitive reservoir is unsubstantiated.
7. Models of mantle convection support tomographic models but reveal a strongly mixed convecting mantle with enriched and depleted lithologies formed by partial melting processes at Earth's surface. Early deep isolated reservoirs are likely to exist but are relatively minor features of the present-day mantle. A more remarkable feature is the presence of strongly refractory material throughout the mantle, and focus on these noble gas, radiogenic and stable isotope attributes of such a reservoir are required for a fuller understanding of mantle processes.

8. Finally, determining the relationship of primordial compositions determined with noble gases, with volatile elements including carbon, hydrogen, nitrogen and sulfur are important in OIB studies. How the noble gases correlate the C-H-N-S is likely to provide details not only on the the differentiation and evolution of mantle endmembers, but also on the accretion and volatile history of the Earth.

Acknowledgements

David (Dave) R. Hilton was instrumental in the first author's journey in science. From hosting him as a PhD student, to eventually welcoming him as a colleague, Dave never faltered in his support and generosity. Dave, you are sorely missed. Support for this work came from the National Science Foundation EAR Grant #1918322 "A mixed-up mantle beneath Ocean Islands?". We are grateful to two reviewers, the guest editor, Justin Kulongoski and Don Porcelli for their constructive comments.

References

Aldrich, L.T., Nier, A.O., 1946. The abundance of He 3 in atmospheric and well helium. Physical Review, 70, 983.

Alvarez, L.W., Cornog, R., 1939. Helium and hydrogen of mass 3. Physical Review, 56, 613.

Allègre, C.J., Turcotte, D.L., 1986. Implications of a two-component marble-caked mantle. Nature 323, 123-127.

Allègre, C.J., Staudacher, T., Sarda, P., Kurz, M., 1983. Constraints on evolution of Earth's mantle from rare gas systematics. Nature, 303, 762-766.

Ammon, K., Dunai, T.J., Stuart, F.M., Meriaux, A.S., Gayer, E., 2009. Cosmogenic ^{3}He exposure ages and geochemistry of basalts from Ascension Island, Atlantic Ocean. Quaternary Geochronology, 4, 525-532.

Basu, A.R., Poreda, R.J., Renne, P.R., Teichmann, F., Vasiliev, Y.R., Sobolev, N.V., Turrin, B.D., 1995. High-^{3}He plume origin and temporal-spatial evolution of the Siberian flood basalts. Science, 269, 822-825.

Benkert, J.P., Baur, H., Signer, P., Wieler, R., 1993. He, Ne, and Ar from the solar wind and solar energetic particles in lunar ilmenites and pyroxenes. Journal of Geophysical Research 98, 13147–13162.

Black, D.C., Pepin, R.O., 1969. Trapped neon in meteorites—II. Earth and Planetary Science Letters, 6, 395-405.

Brandon, A.D., Norman, M.D., Walker, R.J., Morgan, J.W., 1999. ^{186}Os-^{187}Os systematics of Hawaiian picrites. Earth Planet. Sci. Lett. 174, 25-42.

Brandon, A.D., Graham, D.W., Waight, T., Gautason, B., 2007. ^{186}Os and ^{187}Os enrichments and high-^{3}He/^{4}He sources in the Earth's mantle: Evidence from Icelandic picrites. Geochim. Cosmochim. Acta 71, 4570-4591.

936 Breton, T., Nauret, F., Pichat, S., Moine, B., Moreira, M., Rose-Koga, E.F., Auclair, D., Bosq, C.
937 , Wavrant, L.M., 2013. Geochemical heterogeneities within the Crozet hotspot. Earth and
938 Planetary Science Letters, 376, 126-136.
939 Brounce, M., Stolper E., Eiler J., 2017. Redox variations in Mauna Kea lavas, the oxygen fugacity
940 of the Hawaiian plume, and the role of volcanic gases in Earth's oxygenation. Proceedings of
941 the National Academy of Science, 114, 8997-9002.
942 Caffee, M.W., Hudson, G.B., Velsko, C., Huss, G.R., Alexander, E.C., Chivas, A.R., 1999.
943 Primordial noble gases from Earth's mantle: identification of a primitive volatile component.
944 Science, 285, 2115-2118.
945 Castillo, P.R., Scarsi, P., Craig, H., 2007. He, Sr, Nd, and Pb isotopic constraints on the origin of
946 the Marquesas and other linear volcanic chains. Chemical Geology, 240, 205-221.
947 Chauvel, C., Hofmann, A., Vidal, P., 1992. HIMU-EM: The French Polynesian connection. Earth
948 Planet. Sci. Lett. 110, 99-119.
949 Clarke, W.B., Beg, M.A., Craig, H. 1969. Excess ^{3}He in the sea: evidence for terrestrial primordial
950 helium. Earth and Planetary Science Letters, 6, 213-220.
951 Class, C., Goldstein, S.L., 2005. Evolution of helium isotopes in the Earth's mantle. Nature, 436,
952 1101-1112.
953 Class, C., Goldstein, S.L., Stute, M., Kurz, M.D., Schlosser, P., 2005. Grand Comore Island: a
954 well-constrained "low ^{3}He/^{4}He" mantle plume. Earth and Planetary Science Letters, 233, 391-
955 409.
956 Class, C., Goldstein, S. L., Shirey, S. B., 2009. Osmium isotopes in Grande Comore lavas: a new
957 extreme among a spectrum of EM-type mantle endmembers. Earth and Planetary Science
958 Letters, 284, 219-227.
959 Day J.M.D., 2013. Hotspot volcanism and highly siderophile elements. Chemical Geology, 341,
960 50-74.
961 Day, J.M.D., 2016. Evidence against a non-chondritic mantle source for North Atlantic Igneous
962 Province lavas. Chemical Geology, 440, 91-100.
963 Day J.M.D., Hilton D.R., 2011. Origin of ^{3}He/^{4}He ratios in HIMU-type basalts constrained from
964 Canary Island lavas. Earth and Planetary Science Letters, 305, 226-234.
965 Day, J.M.D., Hilton, D.R., 2021. Heterogeneous mantle-derived ^{3}He/^{4}He in the Canary Islands
966 and other ocean islands. Geology, 49, 120-124.
967 Day, J.M.D., Jones, T.D., 2021. Depleted mantle plumes.
968 https://2021.goldschmidt.info/goldschmidt/2021/meetingapp.cgi/Paper/7754
969 Day, J.M.D., Pearson, D.G., Macpherson, C.G., Lowry, D., Carracedo, J.-C., 2009. Pyroxenite-
970 rich mantle formed by recycled oceanic lithosphere: oxygen-osmium isotope evidence from
971 Canary Island lavas. Geology, 37, 555-558.
972 Day J.M.D., Pearson D.G., Macpherson C.G., Lowry D., Carracedo J.-C., 2010. Evidence for
973 distinct proportions of subducted oceanic crust and lithosphere in HIMU-type mantle beneath
974 El Hierro and La Palma, Canary Islands. Geochimica et Cosmochimica Acta, 74, 6565-6589.
975 Day J.M.D., Barry P.H., Hilton D.R., Pearson D.G., Burgess, R., Taylor L.A., 2015. The helium
976 flux from the continents and ubiquity of low-^{3}He/^{4}He recycled crust and lithosphere.
977 Geochimica et Cosmochimica Acta, 153, 116-133.
978 Day, J.M.D., Walker, R.J., Warren, J.M., 2017. ^{186}Os-^{187}Os and highly siderophile element
979 abundance systematics of the mantle revealed by abyssal peridotites and Os-rich alloys.
980 Geochimica et Cosmochimica Acta, 200, 232-254.

Day, J.M.D., Harvey, R.P., Hilton, D.R., 2019. Melt-modified lithosphere beneath Ross Island and its role in the tectono-magmatic evolution of the West Antarctic Rift System. Chemical Geology, 518, 45-54.

Doucet, S., Moreira, M., Weis, D., Scoates, J.S., Giret, A. and Allegre, C., 2006. Primitive neon and helium isotopic compositions of high-MgO basalts from the Kerguelen Archipelago, Indian Ocean. Earth and Planetary Science Letters, 241, 65-79.

Doucelance, R., Escrig, S., Moreira, M., Gariépy, C., Kurz, M.D., 2003. Pb-Sr-He isotope and trace element geochemistry of the Cape Verde Archipelago. Geochimica et Cosmochimica Acta, 67, 3717-3733.

Eiler, J.M., Farley, K.A., Valley, J.W., Hauri, E.H., Craig, H., Hart, S.R., Stolper, E.M., 1997. Oxygen isotope variations in ocean island basalt phenocrysts. Geochimica et Cosmochimica Acta, 61, 2281-2293.

Elliott, T., Blichert-Toft, J., Heumann, A., Koetsier, G. & Forjaz, V., 2007. The origin of enriched mantle beneath São Miguel, Azores. Geochimica et Cosmochimica Acta, 71, 219-240.

Engel, A.J., Engel, C.G., Havens, R.G., 1965. Chemical characteristics of oceanic basalts and the upper mantle. Geological Society of America Bulletin, 76, 719-734.

Farley, K.A., Poreda, R.J., 1993. Mantle neon and atmospheric contamination. Earth and Planetary Science Letters, 114, 325-339.

Farley, K.A., Neroda, E., 1998. Noble gases in the Earth's mantle. Annual Reviews in Earth and Planetary Sciences, 26, 189-218.

Farley, K.A., Natland, J.H. & Craig, H., 1992. Binary mixing of enriched and undegassed (primitive?) mantle components (He, Sr, Nd, Pb) in Samoan lavas. Earth and Planetary Science Letters, 111, 183-199.

Fisher, D.E., 1983. Rare gases from the undepleted mantle?. Nature, 305, 298-300.

French, S.W., Romanowicz, B., 2015. Broad plumes rooted at the base of the Earth's mantle beneath major hotspots. Nature, 525, 95-99.

Füri E., Hilton D.R., Murton B.J., Hemond C., Dyment J., Day J.M.D., 2011. Helium isotope variations between Réunion Island and the Central Indian Ridge (17˚-21˚S): new evidence for ridge-hotspot interaction. Journal of Geophysical Research – Solid Earth, doi:10.1029/2010JB007609 (17 pages).

Füri, E., Hilton, D.R., Halldórsson, S.A., Barry, P.H., Hahm, D., Fischer T.P., Grönvold, K., 2010. Apparent decoupling of the He and Ne isotope systematics of the Icelandic mantle: The role of He depletion, melt mixing, degassing fractionation and air interaction. Geochemica Cosmochimica Acta, 74, 11.

Garapić, G., Mallik, A., Dasgupta, R., Jackson, M.G., 2015. Oceanic lavas sampling the high-$^{3}He/^{4}He$ mantle reservoir: Primitive, depleted, or re-enriched?. American Mineralogist, 100, 2066-2081.

Gast, P.W., Tilton, G.R., Hedge, C., 1964. Isotopic composition of lead and strontium from Ascension and Gough Islands. Science, 145, 1181-1185.

Gibson, S.A., Dale, C.W., Geist, D.J., Day, J.A., Brügmann, G., Harpp, K.S., 2016. The influence of melt flux and crustal processing on Re–Os isotope systematics of ocean island basalts: Constraints from Galápagos. Earth and Planetary Science Letters, 449, 345-359.

Gonnermann, H.M., Mukhopadhyay, S., 2009. Preserving noble gases in a convecting mantle. Nature, 459, 560-563.

Graham, D.W., 2002. Noble gases in MORB and OIB: observational constraints for the characterization of mantle source reservoirs. Reviews in Mineralogy and Geochemistry 46, 247-318.

Graham, D.W., Lupton, F., Albarède, F., Condomines, M., 1990. Extreme temporal homogeneity of helium isotopes at Piton de la Fournaise, Réunion. Nature, 347, 545-548.

Graham, D.W., Johnson, K.T.M., Priebe, L.D., Lupton, J.E., 1999. Hotspot–ridge interaction along the Southeast Indian Ridge near Amsterdam and St. Paul islands: helium isotope evidence. Earth and Planetary Science Letters, 167, 297-310.

Gurenko, A.A., Hoernle, K.A., Hauff, F., Schmincke, H.-U., Han, D., Miura, Y.N., Kaneoka, I., 2006. Major, trace element and Nd–Sr–Pb–O–He–Ar isotope signatures of shield stage lavas from the central and western Canary Islands: insights into mantle and crustal processes. Chemical Geology 233, 75-112.

Hanan, B.B., Graham, D.W., 1996. Lead and helium isotope evidence from oceanic basalts for a common deep source of mantle plumes. Science, 272, 991-995.

Hanyu, T., 2014. Deep plume origin of the Louisville hotspot: Noble gas evidence. Geochemistry, Geophysics, Geosystems, 15, 565-576.

Hanyu, T., Kaneoka, I., 1997. The uniform and low $^{3}He/^{4}He$ ratios of HIMU basalts as evidence for their origin as recycled materials. Nature, 390, 273-276.

Hanyu, T., Kaneoka, I., Nagao, K., 1999. Noble gas study of HIMU and EM ocean island basalts in the Polynesian region. Geochimica et Cosmochimica Acta, 63, 1181-1201.

Hanyu, T., Dunai, T.J., Davies, G.R., Kaneoka, I., Nohda, S., Uto, K., 2001. Noble gas study of the Reunion hotspot: evidence for distinct less-degassed mantle sources. Earth and Planetary Science Letters, 193, 83-98.

Hanyu, T., Tatsumi, Y., Kimura, J.I., 2011. Constraints on the origin of the HIMU reservoir from He–Ne–Ar isotope systematics. Earth and Planetary Science Letters, 307, 377-386.

Harðardóttir, S., Halldórsson, S.A., Hilton, D.R., 2018. Spatial distribution of helium isotopes in Icelandic geothermal fluids and volcanic materials with implications for location, upwelling and evolution of the Icelandic mantle plume. Chemical Geology, 480, 12-27.

Harper Jr, C.L., Jacobsen, S.B., 1996. Noble gases and Earth's accretion. Science, 1814-1818.

Hart, S. R., Hauri, E. H., Oschmann, L. A., Whitehead, J. A., 1992. Mantle plumes and entrainment: isotopic evidence. Science, 256 517-520.

Hart, S.R., Coetzee, M., Workman, R.K., Blusztajn, J., Johnson, K.T.M., Sinton, J.M., Steinberger, B., Hawkins, J.W., 2004. Genesis of the Western Samoa seamount province: age, geochemical fingerprint and tectonics. Earth and Planetary Science Letters, 227, 37-56.

Heber, V.S., Wieler, R., Baur, H., Olinger, C., Friedmann, T.A., Burnett, D.S., 2009. Noble gas composition of the solar wind as collected by the Genesis mission. Geochimica et Cosmochimica Acta, 73, 7414-7432.

Heber, V.S., Baur, H., Bochsler, P., McKeegan, K.D., Neugebauer, M., Reisenfeld, D.B., Wieler, R., Wiens, R.C., 2012. Isotopic mass fractionation of solar wind: Evidence from fast and slow solar wind collected by the Genesis mission. The Astrophysical Journal, 759, 121.

Helz, R. T., Cottrell, E., Brounce, M. N., Kelley, K. A. 2017. Olivine-melt relationships and syneruptive redox variations in the 1959 eruption of Kilauea Volcano as revealed by XANES. Journal of Volcanology and Geothermal Research.

Hennecke, E.W. and Manuel, O.K., 1975. Noble gases in an Hawaiian xenolith. Nature, 257, 778-780.

Hilton, D.R., Hammerschmidt, K., Teufel, S., Freidrichsen, H., 1993. Helium isotope characteristics of Andean geothermal fluids and lavas, Earth and Planetary Science Letters 120, 265-282.

Hilton, D.R., McMurtry, G.M. & Kreulen, R., 1997. Large variations in vent fluid $CO_2/^3He$ ratios signal rapid changes in magma chemistry at Loihi seamount, Hawaii. Nature, 396, 359-362.

Hilton, D.R., Barling, J., Wheller, G.E., 1995. Effect of shallow-level contamination on the helium isotope systematics of ocean-island lavas. Nature, 373, 330-333.

Hilton, D. R., Grönvold, K., Macpherson, C. G., Castillo, P. R., 1999. Extreme $^3He/^4He$ ratios in northwest Iceland: constraining the common component in mantle plumes. Earth and Planetary Science Letters, 173, 53-60.

Hilton, D.R., Macpherson C.G., Elliott, T.R., 2000. Helium isotope ratios in mafic phenocrysts and geothermal fluids from La Palma, the Canary Islands (Spain): Implications for HIMU mantle sources. Geochimica et Cosmochimica Acta 64, 2119-2132.

Hilton, D.R., Halldórsson, S.A., Barry, P.H., Fischer, T.P., de Moor, J.M., Ramirez, C.J., Mangasini, F., Scarsi, P., 2011. Helium isotopes at Rungwe Volcanic Province, Tanzania, and the origin of East African plateaux. Geophysical Research Letters, 38(21).

Hoernle, K., Tilton, G., Schmincke, H.U., 1991. Sr-Nd-Pb isotopic evolution of Gran Canaria: Evidence for shallow enriched mantle beneath the Canary Islands. Earth and Planetary Science Letters, 106, 44-63.

Hofmann, A.W., 1997. Mantle geochemistry: the message from oceanic volcanism. Nature, 385, 219-229.

Hofmann, A.W., White, W.M., 1982. Mantle plumes from ancient oceanic crust. Earth and Planetary Science Letters 57, 421-436.

Hoggard, M.J., Parnell-Turner, R., White, N., 2020. Hotspots and mantle plumes revisited: Towards reconciling the mantle heat transfer discrepancy. Earth and Planetary Science Letters, 542, 116317.

Holland, G., Ballentine, C.J., 2006. Seawater subduction controls the heavy noble gas composition of the mantle. Nature, 441, 186-191.

Honda, M., Woodhead, J.D., 2005. A primordial solar-neon enriched component in the source of EM-I-type ocean island basalts from the Pitcairn Seamounts, Polynesia. Earth and Planetary Science Letters, 236, 597-612.

Honda, M., McDougall, I., Patterson, D.B., Doulgeris, A., Clague, D.A., 1991. Possible solar noble-gas component in Hawaiian basalts. Nature, 349, 149-151.

Horton, F., Farley, K., Jackson, M., 2019. Helium distributions in ocean island basalt olivines revealed by X-ray computed tomography and single-grain crushing experiments. Geochimica et Cosmochimica Acta, 244, 467-477.

Honda, M., McDougall, I., Patterson, D., 1993. Solar noble gases in the Earth: the systematics of helium-neon isotopes in mantle derived samples. Lithos, 30, 257-265.

Jackson M. G., Kurz M. D., Hart S. R., Workman R. K., 2007. New Samoan lavas from Ofu Island reveal a hemispherically heterogeneous high 3He/4He mantle. Earth and Planetary Science Letters, 264, 360–374.

Jackson, M.G., Kurz, M.D., Hart, S.R., 2009. Helium and neon isotopes in phenocrysts from Samoan lavas: Evidence for heterogeneity in the terrestrial high $^3He/^4He$ mantle. Earth and Planetary Science Letters, 287, 519-528.

Jackson, M.G., Carlson, R.W., Kurz, M.D., Kempton, P.D., Francis, D., Blusztajn, J., 2010. Evidence for the survival of the oldest terrestrial mantle reservoir. Nature, 466, 853-856.

Jackson, M. G., Shirey, S. B., 2011. Re–Os isotope systematics in Samoan shield lavas and the use of Os-isotopes in olivine phenocrysts to determine primary magmatic compositions. Earth and Planetary Science Letters, 312, 91-101.

Jackson, M.G., Hart, S.R., Konter, J.G., Kurz, M.D., Blusztajn, J., Farley, K.A., 2014. Helium and lead isotopes reveal the geochemical geometry of the Samoan plume. Nature, 514, 355-358.

Jackson M. G., Konter, J. G., Becker, T. W., 2017. Primordial helium entrained by the hottest mantle plumes. Nature 542: 340-343.

Jackson, M.G., Price, A.A., Blichert-Toft, J., Kurz, M.D., Reinhard, A.A., 2017. Geochemistry of lavas from the Caroline hotspot, Micronesia: Evidence for primitive and recycled components in the mantle sources of lavas with moderately elevated $^{3}He/^{4}He$. Chemical Geology, 455, 385-400.

Jackson, M.G., Blichert-Toft, J., Halldórsson, S.A., Mundl-Petermeier, A., Bizimis, M., Kurz, M.D., Price, A.A., Harðardóttir, S., Willhite, L.N., Breddam, K. and Becker, T.W., 2020. Ancient helium and tungsten isotopic signatures preserved in mantle domains least modified by crustal recycling. Proceedings of the National Academy of Sciences, 117, 30993-31001.

Jean-Baptiste, P., Allard, P., Coutinho, R., Ferreira, T., Fourré, E., Queiroz, G., Gaspar, J.L., 2009. Helium isotopes in hydrothermal volcanic fluids of the Azores archipelago. Earth and Planetary Science Letters, 281, 70-80.

Jones, T. D., Davies, D. R., Sossi, P. A., 2019. Tungsten Isotopes in Mantle Plumes: Heads it's Positive Tails it's Negative Earth and Planetary Science Letters, 506, 255-267.

Jones, T. D., Maguire, R. R., van Keken, P. E., Ritsema, J., Koelemeijer, P., 2020. Subducted oceanic crust as the origin of seismically slow lower-mantle structures. Progress in Earth and Planetary Science, 7, 17. https://doi.org/10.31223/osf.io/k98p7

Kaneoka, I., 1983. Noble gas constraints on the layered structure of the mantle. Nature, 302, 698-700.

Kaneoka, I. and Takaoka, N., 1978. Excess ^{129}Xe and high $^{3}He/^{4}He$ ratios in olivine phenocrysts of Kapuho lava and xenolithic dunites from Hawaii. Earth and Planetary Science Letters, 39, 382-386.

Kendrick, M.A., Scambelluri, M., Honda, M., Phillips, D., 2011. High abundances of noble gas and chlorine delivered to the mantle by serpentinite subduction. Nature Geoscience, 4, 807-812.

Kendrick, M.A., Scambelluri, M., Hermann, J., Padrón-Navarta, J.A., 2018. Halogens and noble gases in serpentinites and secondary peridotites: Implications for seawater subduction and the origin of mantle neon. Geochimica et cosmochimica acta, 235, 285-304.

Kurz, M.D., Jenkins, W.J., Hart, S.R., 1982. Helium isotopic systematics of oceanic islands and mantle heterogeneity. Nature, 297, 43-47.

Kurz, M.D., Kenna, T.C., Lassiter, J.C., DePaolo, D.J., 1996. Helium isotopic evolution of Mauna Kea volcano: First results from the 1-km drill core. Journal of Geophysical Research: Solid Earth, 101(B5), 11781-11791.

Kurz, M.D., le Roex, A.P., Dick, H.J., 1998. Isotope geochemistry of the oceanic mantle near the Bouvet triple junction. Geochimica et Cosmochimica Acta, 62, 841-852.

Kurz, M.D., Moreira, M., Curtice, J., Lott III, D.E., Mahoney, J.J., Sinton, J.M., 2005. Correlated helium, neon, and melt production on the super-fast spreading East Pacific Rise near 17 S. Earth and Planetary Science Letters, 232, 125-142.

Kurz, M.D., Curtice, J., Fornari, D., Geist, D., Moreira, M., 2009. Primitive neon from the center of the Galápagos hotspot. Earth and Planetary Science Letters, 286, 23-34.

Lupton, J.E., Craig, H., 1975. Excess ^{3}He in oceanic basalts: evidence for terrestrial primordial helium. Earth and Planetary Science Letters, 26, 133-139.

Lupton, J.E., Graham, D.W., Delaney, J.R, Johnson, H.P., 1993. Helium isotope variations in Juan de Fuca Ridge basalts. Geophysical Research Letters, 20, 1851-1854.

Lupton, J.E., Arculus, R.J., Evans, L.J., Graham, D.W., 2012. Mantle hotspot neon in basalts from the Northwest Lau Back-arc Basin. Geophysical research letters, 39(8).

Macpherson C.G., Hilton D.R., Day J.M.D., Lowry D., Grönvold K., 2005. High-^{3}He/^{4}He depleted mantle and low-δ^{18}O recycled oceanic lithosphere in the source of central Icelandic lavas. Earth and Planetary Science Letters, 233, 411-427.

Madureira, P., Moreira, M., Mata, J., Allègre, C.J., 2005. Primitive neon isotopes in Terceira Island (Azores archipelago). Earth and Planetary Science Letters, 233, 429-440.

Mamyrin, B.A., 1969. Anomalous isotopic composition of helium in volcanic gases. In Dokl. Akad. Nauk SSSR (Vol. 184, pp. 1197-1199).

Marty, B., 2020. Origins and early evolution of the atmosphere and oceans. Geochemical Perspectives, 9, 1-313.

Mata, J., Moreira, M., Doucelance, R., Ader, M., Silva, L.C., 2010. Noble gas and carbon isotopic signatures of Cape Verde oceanic carbonatites: implications for carbon provenance. Earth and Planetary Science Letters, 291, 70-83.

Meisel, T., Walker, R.J., Morgan, J.W., 1996. The osmium isotopic composition of the Earth's primitive upper mantle. Nature, 383, 517-520.

Moreira, M., 2013. Noble gas constraints in the origin and evolution of Earth's volatiles. Geochemical Perspectives, 2, 1-403.

Moreira, M., Kurz, M.D., 2001. Subducted oceanic lithosphere and the origin of the 'high μ' basalt helium isotopic signature. Earth and Planetary Science Letters, 189, 49-57.

Moreira, M., Allègre, C., 2004. Helium isotopes on the Macdonald seamount (Austral chain): constraints on the origin of the superswell. Comptes Rendus Géoscience, 336, 983-990.

Moreira, M., Madureira, P., 2005. Cosmogenic helium and neon in 11 Myr old ultramafic xenoliths: consequences for mantle signatures in old samples. Geochemistry, Geophysics, Geosystems, 6(8).

Moreira, M.,Charnoz, S., 2016. The origin of the neon isotopes in chondrites and on Earth. Earth and Planetary Science Letters, 433, 249-256.

Moreira, M., Kunz, J., Allegre, C., 1998. Rare gas systematics in popping rock: isotopic and elemental compositions in the upper mantle. Science, 279, 1178-1181.

Moreira, M., Breddam, K., Curtice, J., Kurz, M.D., 2001. Solar neon in the Icelandic mantle: new evidence for an undegassed lower mantle. Earth and Planetary Science Letters, 185, 15-23.

Moreira, M., Doucelance, R., Kurz, M.D., Dupré, B., Allègre, C.J., 1999. Helium and lead isotope geochemistry of the Azores Archipelago. Earth and Planetary Science Letters, 169, 189-205.

Moriera, M., Kanzari, A., Madureira, P., 2012. Helium and neon isotopes in São Miguel island basalts, Azores Archipelago: new constraints on the "low ^{3}He" hotspot origin. Chemical Geology, 322-323, 91-98.

Moussallam, Y., Oppenheimer, C., Scaillet, B., Gaillard, F., Kyle, P., Peters, N., Hartley, M., Berlo, K., Donovan, A., 2014. Tracking the changing oxidation state of Erebus magmas, from mantle to surce, driven magma ascent and degassing. Earth and Planetary Science Letters 393: 200-209.

Moussallam, Y., Edmonds, M., Scaillet, B., Peters, N., Gennaro, E., Sides, I., Oppenheimer, C. 2016. The impact of degassing on the oxidation state of basaltic magmas: A case study of Kilauea volcano. Earth and Planetary Science Letters 450: 317-325.

Moussallam, Y., Longpré, M.A., McCammon, C., Gomez-Ulla, A., Rose-Koga, E.F., Scaillet, B., Peters, N., Gennaro, E., Paris, R., Oppenheimer, C., 2019. Mantle plumes are oxidised. Earth and Planetary Science Letters, 527, 115798.

Mukhopadhyay, S., Parai, R., 2019. Noble gases: a record of Earth's evolution and mantle dynamics. Annual Review of Earth and Planetary Sciences, 47, 389-419.

Mundl, A., Touboul, M., Jackson, M.G., Day, J.M.D., Kurz, M.D., Lekic, V., Helz, R.T., Walker, R.J., 2017. 182-W isotope heterogeneity in modern ocean island basalts. Science, 356, 66-69.

Mundl-Petermeier, A., Walker, R.J., Jackson, M.G., Blichert-Toft, J., Kurz, M.D., Halldórsson, S.A., 2019. Temporal evolution of primordial tungsten-182 and $^{3}He/^{4}He$ signatures in the Iceland mantle plume. Chemical Geology, 525, 245-259.

Mundl-Petermeier A., Walker, R. J., Fischer, R. A., Lekic, V., Jackson, M. G., Kurz, M. D., 2020. Anomalous ^{182}W in high $^{3}He/^{4}He$ ocean island basalts: Fingerprints of Earth's core? Geochimica et Cosmochimica Acta 271: 194-211.

Nicklas R. W., Puchtel I. S., Ash R. D., Piccoli P. M., Hanski E., Nisbet E. G., Waterton P, M., Pearson D. G., Anbar A. D., 2019. Secular Mantle Oxidation across the Archean-Proterozoic Boundary: Evidence from V Partitioning in Komatiites and Picrites. Geochimica et Cosmochimica Acta 250: 49-75.

Nicklas, R. W., Brandon, A.D., Waight, T.E., Puchtel, I.S., Day, J.M.D., 2021. High-precision Pb and Hf isotope and highly siderophile element abundance systematics of high-MgO Icelandic lavas. Chemical Geology, 582, 120436.

Niedermann, S., Graf, T., Marti, K., 1993. Mass spectrometric identification of cosmic-ray produced neon in terrestrial rocks with multiple neon components. Earth Planetary Science Letters 118, 65–73.

Niedermann, S., Bach, W.,Erzinger, J., 1997. Noble gas evidence for a lower mantle component in MORBs from the southern East Pacific Rise: Decoupling of helium and neon isotope systematics. Geochimica et Cosmochimica Acta, 61, 2697-2715.

Ozima, M., Podosek, F.A., 2002. Noble gas geochemistry. Cambridge University Press.

Parai, R., Mukhopadhyay, S., 2015. The evolution of MORB and plume mantle volatile budgets: Constraints from fission Xe isotopes in Southwest Indian Ridge basalts. Geochemistry, Geophysics, Geosystems, 16, 719-735.

Parai, R., Mukhopadhyay, S., 2021. Heavy noble gas signatures of the North Atlantic Popping Rock 2ΠD43: Implications for mantle noble gas heterogeneity. Geochimica et Cosmochimica Acta. 294, 89-105.

Parai, R., Mukhopadhyay, S., Lassiter, J.C., 2009. New constraints on the HIMU mantle from neon and helium isotopic compositions of basalts from the Cook-Austral Islands. Earth and Planetary Science Letters, 277, 253-261.

Parai, R., Mukhopadhyay, S., Standish, J.J., 2012. Heterogeneous upper mantle Ne, Ar and Xe isotopic compositions and a possible Dupal noble gas signature recorded in basalts from the Southwest Indian Ridge. Earth and Planetary Science Letters, 227-239.

Parai, R., Mukhopadhyay, S., Tucker, J.M., Pető, M.K., 2019. The emerging portrait of an ancient, heterogeneous and continuously evolving mantle plume source. Lithos, 346, 105153.

Paquet, M., Day, J.M.D., Castillo, P., 2019. Osmium isotope evidence for a heterogeneous $^{3}He/^{4}He$ mantle plume beneath the Juan Fernandez Islands. Geochimica et Cosmochimica Acta. 261, 1-19.

Péron, S., Moreira, M., Colin, A., Arbaret, L., Putlitz, B., Kurz, M.D., 2016. Neon isotopic composition of the mantle constrained by single vesicle analyses. Earth and Planetary Science Letters, 449, 145-154.

Péron, S., Moreira, M., Putlitz, B., Kurz, M.D., 2017. Solar wind implantation supplied light volatiles during the first stage of Earth accretion. Geochemical Perspectives Letters, 3, 151-159.

Péron, S., Moreira, M., Agranier, A., 2018. Origin of light noble gases (He, Ne, and Ar) on Earth: A review. Geochemistry, Geophysics, Geosystems, 19(4), 979-996.

Peters, B.J., Mundl-Petermeier, A., Carlson, R.W., Walker, R.J., Day, J.M.D., 2021. Combined lithophile-siderophile isotopic constraints on Hadean processes preserved in ocean island basalt sources. Geochemistry, Geophysics, Geosystems, 22, e2020GC009479.

Pető, M.K., Mukhopadhyay, S., Kelley, K.A., 2013. Heterogeneities from the first 100 million years recorded in deep mantle noble gases from the Northern Lau Back-arc Basin. Earth and Planetary Science Letters, 369, 13-23.

Poreda, R.J., Schilling, J.G., Craig, H., 1993. Helium isotope ratios in Easter microplate basalts. Earth and Planetary Science Letters, 119, 319-329.

Raquin, A., Moreira, M., 2009. Atmospheric $^{38}Ar/^{36}Ar$ in the mantle: implications for the nature of the terrestrial parent bodies. Earth and Planetary Science Letters, 287, 551-558.

Sarda, P., Staudacher, T., Allegre, C.J., 1988. Neon isotopes in submarine basalts. Earth and Planetary Science Letters, 91, 73-88.

Sarda, P., Moreira, M., Staudacher, T., Schilling, J.G., Allègre, C.J., 2000. Rare gas systematics on the southernmost Mid-Atlantic Ridge: Constraints on the lower mantle and the Dupal source. Journal of Geophysical Research: Solid Earth, 105(B3), 5973-5996.

Scarsi, P., 2000. Fractional extraction of helium by crushing of olivine and clinopyroxene phenocrysts: Effects on the 3He/4He measured ratio. Geochimica et Cosmochimica Acta. 64, 3751-3762.

Sedwick, P.N., McMurtry, G.M., Hilton, D.R., Goff, F., 1994. Carbon dioxide and helium in hydrothermal fluids from Loihi Seamount, Hawaii, USA: temporal variability and implications for the release of mantle volatiles. Geochimica et Cosmochimica Acta, 58, 1219-1227.

Shaw, A.M., Hilton, D.R., Macpherson, C.G., Sinton, J.M., 2001. Nucleogenic neon in high $^{3}He/^{4}He$ lavas from the Manus back-arc basin: a new perspective on He–Ne decoupling. Earth and Planetary Science Letters, 194, 53-66.

Staudacher, T., Allègre, C.J., 1988. Recycling of oceanic crust and sediments: the noble gas subduction barrier. Earth and Planetary Science Letters, 89, 173-183.

Staudacher, T., Sarda, P., Allègre, C.J., 1990. Noble gas systematics of Réunion island, Indian Ocean. Chemical Geology, 89, 1-17.

Stracke, A., Zindler, A., Salters, V.J., McKenzie, D., Blichert-Toft, J., Albarède, F., Grönvold, K., 2003. Theistareykir revisited. Geochemistry, Geophysics, Geosystems, 4(2).

Stracke, A., Genske, F., Berndt, J., Koornneef, J.M., 2019. Ubiquitous ultra-depleted domains in Earth's mantle. Nature Geoscience, 12, 851-855.

Stronik, N.A., Krienitz, M-S., Niedermann, S., Romer, R.L., Harris, C., Trumbull, R.B., Day, J.M.D., 2017. Helium isotope evidence for a deep-seated mantle plume involved in South Atlantic break-up. Geology, 45, 827-830.

Taran, Y.A., Inguaggiato, S., Varley, N., Capasso, G.,Favara, R., 2002. Helium and carbon isotopes in thermal waters of the Jalisco block, Mexico. Geofisica Internacional.

Trieloff, M., Kunz, J., Clague, D.A., Harrison, D., Allègre, C.J., 2000. The nature of pristine noble gases in mantle plume. Science. 288, 1036-1038.

Trieloff, M., Kunz, J., Allègre, C.J., 2002. Noble gas systematics of the Réunion mantle plume source and the origin of primordial noble gases in Earth's mantle. Earth and Planetary Science Letters, 200, 297-313.

Troung, T., Castillo, P.R., Hilton, D.R., Day, J.M.D., 2018. The trace element and Sr-Nd-Pb isotope geochemistry of Juan Fernandez lavas as probe of variable contributions from a high-$^{3}He/^{4}He$ mantle plume. Chemical Geology, 476, 280-291.

Trull, T.W., Kurz, M.D., 1993. Experimental measurements of 3He and 4He mobility in olivine and clinopyroxene at magmatic temperatures. Geochimica et Cosmochimica Acta 57, 1313-1324.

Tucker, J.M., Mukhopadhyay, S., Schilling, J.G., 2012. The heavy noble gas composition of the depleted MORB mantle (DMM) and its implications for the preservation of heterogeneities in the mantle. Earth and Planetary Science Letters, 355, 244-254.

Wetherill, G.W., 1954. Variations in the isotopic abundances of neon and argon extracted from radioactive minerals. Physical Review, 96, 679.

Williams, C.D., Mukhopadhyay, S., 2019. Capture of nebular gases during Earth's accretion is preserved in deep-mantle neon. Nature, 565, 78-81.

Williams, C.D., Mukhopadhyay, S., Rudolph, M.L., Romanowicz, B., 2019. Primitive helium is sourced from seismically slow regions in the lowermost mantle. Geochemistry, Geophysics, Geosystems, 20, 4130-4145.

Woodhead, J.D., 1996. Extreme HIMU in an oceanic setting: the geochemistry of Mangaia island (Polynesia), and temporal evolution of the Cook-Austral hotspot. Journal of Volcanology and Geothermal Research, 72, 1-19.

Xie, S., Tackley, P.J., 2004. Evolution of helium and argon isotopes in a convecting mantle. Physics of the Earth and Planetary Interiors, 146, 417-439.

Valbracht, P.J., Staudacher, T., Malahoff, A., Allegre, C.J., 1997. Noble gas systematics of deep rift zone glasses from Loihi Seamount, Hawaii. Earth and Planetary Science Letters, 150, 399-411.

Valbracht, P.J., Honda, M., Matsumoto, T., Mattielli, N., McDougall, I., Ragettli, R., Weis, D., 1996. Helium, neon and argon isotope systematics in Kerguelen ultramafic xenoliths: implications for mantle source signatures. Earth and Planetary Science Letters, 138, 29-38.

Vance, D., Stone, J.O.H., O'Nions, R.K., 1989. He, Sr and Nd isotopes in xenoliths from Hawaii and other oceanic islands. Earth and Planetary Science Letters, 96, 147–160.

Van Keken, P.E., Ballentine, C.J., 1998. Whole-mantle versus layered mantle convection and the role of a high-viscosity lower mantle in terrestrial volatile evolution. Earth and Planetary Science Letters, 156, 19-32.

Yatsevich, I., Honda, M., 1997. Production of nucleogenic neon in the Earth from natural radioactive decay. Journal of Geophysics, 102, 10291-10298.

Yokochi, R., Marty, B., 2004. A determination of the neon isotopic composition of the deep mantle. Earth and Planetary Science Letters, 225, 77-88.

Zahnle, K.J., Gacesa, M., Catling, D.C., 2019. Strange messenger: a new history of hydrogen on Earth, as told by xenon. Geochimica et Cosmochimica Acta, 244, 56-85.

1340 Zindler, A., Hart, S.R., 1986. Chemical geodynamics. Annual Reviews in Earth and Planetary
1341 Science, 14, 493-571.

1342
1343 **Table 1**
1344

Table 1: Properties and isotopic compositions in the atmopshere and Solar components of He, Ne, Ar and Xe.

Element	Stable isotopes	Radiogenic Production	Natural Abundance Atm. (Mole fraction)	Atmopsheric Abundance ppmv	Popping rock (mantle?) ppmv		Ratio in Atmosphere	Ratio in Solar Wind
Helium	^{3}He		1.3359E-06			^{4}He/^{3}He	748570	~2500
	^{4}He		1.0000	5.24	~2.9	^{3}He/^{4}He (R/R$_A$)	1	~290
Neon	^{20}Ne		0.9048	18.2	0.008	^{20}Ne/^{22}Ne	9.8	13.8
	^{21}Ne	^{18}O or ^{24}Mg (n,α)^{21}Ne	0.0027			^{21}Ne/^{22}Ne	0.029	0.034
	^{22}Ne		0.0925					
Argon	^{36}Ar		0.0003			^{38}Ar/^{36}Ar	0.188	0.1818
	^{38}Ar		0.0001			^{40}Ar/^{36}Ar	296	
	^{40}Ar	Electron capture ^{40}K	0.9960	9340	1			
Xenon	^{124}Xe		0.0010	0.087	0.0001	^{124}Xe/^{130}Xe	0.0234	0.0294
	^{126}Xe		0.0009			^{126}Xe/^{130}Xe	0.0218	0.0255
	^{128}Xe		0.0191			^{128}Xe/^{130}Xe	0.471	0.51
	^{129}Xe	β-decay ^{129}I (15.7 Ma)	0.2640			^{129}Xe/^{130}Xe	6.5	6.27
	^{130}Xe		0.0407			^{131}Xe/^{130}Xe	5.21	4.98
	^{131}Xe	SF ^{244}Pu (80 Ma) + ^{238}U	0.2123			^{132}Xe/^{130}Xe	6.61	6.02
	^{132}Xe	SF ^{244}Pu (80 Ma) + ^{238}U	0.2690			^{134}Xe/^{130}Xe	2.56	2.21
	^{134}Xe	SF ^{244}Pu (80 Ma) + ^{238}U	0.1043			^{136}Xe/^{130}Xe	2.18	1.8
	^{136}Xe	SF ^{244}Pu (80 Ma) + ^{238}U	0.0885					

SF = Spontaneous fission. Ratio and abundance data are from Heber et al. (2009), Moreira (2013), Parai & Mukhopadhyay (2021), and references therein.

1345

1346 **Table 2**

Table 2: Helium, neon, argon and xenon systematics known for OIB (note, in all cases, the range of $^{3}He/^{4}He$ in OIB archipelagos ranges well maximum values reported).

	$^{3}He/^{4}He$ (R/R_A)	$^{3}He/^{4}He$ (R/R_A)	$^{21}Ne/^{22}Ne_{Ext}$	$^{40}Ar/^{36}Ar_{Ext}$	$^{129}Xe/^{130}Xe_{Ext}$	Plume Buoyancy (Mg s^{-1})	Plume Buoyancy (Mg s^{-1})
Source	a	b				c	a
Iceland (NW Iceland/DICE)	37.7	37.7	0.0374	10750	7.0	4.07	1.52
Hawaii (Loihi)	35.3	35.3	0.040	8000	6.6	2.78	4.9
Samoa (Ofu)	33.8	33.8	0.038			2.23	1.2
Samoe (Rochambeau)	28.1	28.1	0.0423	16763	6.9	2.23	1.2
Samoa (Savaii)	4.4					2.23	1.2
Galapagos (Fernandina)	30.3	30.3	0.035	6500	6.9	1.88	0.33
Easter	26	11.3				0.06	0.7
Azores (Terceira)	18.4	14.8	0.052			0.9	0.38
Azores (Sao Miguel)	3.7		0.041			0.9	0.38
Heard/Kerguelen	18.3	18.3	0.044				0.73
Juan Fernandez	17.2	18				1.15	0.2
Societies	17.0	17.0					1.86
Macdonald	15.8	15.8	0.052			0.63	1.18
Cape Verde	15.7	15.7				2.36	0.32
Discovery	15.2	15.2				0.43	0.04
Bouvet	14.9	15				0.37	0.06
Marquesas	14.4	14.4				0.88	0.55
Amsterdam and St. Paul Islands	14.1	14.1					0.02
Crozet	14.0					1.2	0.25
Reunion	13.6	14.5	0.042			2.02	0.07
Caroline	12.8	12.8				0.99	0.85
Pitcairn	12.6	13.4	0.034			0.29	0.45
Meteor/Shona	12.3	12.4				0.37	0.03
Louisville	10.6	10.6				0.19	0.6
Canary Islands (La Palma)	9.7	9.7	0.037			0.93	0.29
Canary Islands (El Hierro)	8.2		0.030			0.93	0.29
Hoggar	8.9					0.23	0.25
Cobb (Axial Smt.)/Juan de Fuca	8.8	8.8				0.51	0.12
Jan Mayen	8.1						0.21
Marion/Prince Edward	7.4	7.9				1.16	0.01
Ascension	7.3	7.3				0.36	0.11
Comores	7.1	7.2				1.04	0.07
Tristan/Gough/Walvis Ridge[e]	7.0	7.1				0.4	0.27
St Helena	6.0	5.9				0.4	0.03
Baja/Guadalupe	5.8	5.8					0.01
MORB	~6-10	~6-10	0.059-0.068	18100-49000	6.9-7.8	-	-

Sources of data for maximum He isotope values from (a) Jackson et al. (2017) and (b) Williams et al. (2019). Plume buoyancy fluxes are from (a) and (c) Hoggard et al. (2020). Extrapolated Ne, Ar, Xe data are calculated or used from Treiloff et al. (2000), Jackson et al. (2009), Mukhopadhyay (2012), Peto et al. (2013), Peron et al. (2017) and Parai et al. (2019).

1347